



LUND UNIVERSITY

Lectures on System Identification - Frequency Response Analysis

Åström, Karl Johan

1975

Document Version:

Publisher's PDF, also known as Version of record

[Link to publication](#)

Citation for published version (APA):

Åström, K. J. (1975). *Lectures on System Identification - Frequency Response Analysis*. (Research Reports TFRT-3093). Department of Automatic Control, Lund Institute of Technology (LTH).

Total number of authors:

1

General rights

Unless other specific re-use rights are stated the following general rights apply:

Copyright and moral rights for the publications made accessible in the public portal are retained by the authors and/or other copyright owners and it is a condition of accessing publications that users recognise and abide by the legal requirements associated with these rights.

- Users may download and print one copy of any publication from the public portal for the purpose of private study or research.
- You may not further distribute the material or use it for any profit-making activity or commercial gain
- You may freely distribute the URL identifying the publication in the public portal

Read more about Creative commons licenses: <https://creativecommons.org/licenses/>

Take down policy

If you believe that this document breaches copyright please contact us providing details, and we will remove access to the work immediately and investigate your claim.

LUND UNIVERSITY

PO Box 117
221 00 Lund
+46 46-222 00 00

REPORT 7504

FEBRUARY 1975



Lectures on System Identification

Chapter 3

Frequency Response Analysis

K.J. ÅSTRÖM

K.J. ÅSTRÖM • LECTURES ON SYSTEM IDENTIFICATION CHAPTER 3 FREQUENCY RESPONSE ANALYSIS



Department of Automatic Control • Lund Institute of Technology

LECTURES ON SYSTEM IDENTIFICATION

Chapter 3: FREQUENCY RESPONSE ANALYSIS.

K. J. Åström

TABLE OF CONTENTS	<u>Page</u>
1. INTRODUCTION	1
2. A DIRECT APPROACH	4
Submarine Dynamics	8
Pupillary Light Reflex Dynamics	15
Unstable Systems	21
Nonlinear Systems	23
Exercises	25
3. THE CORRELATION METHOD	29
Analysis	30
Frequency Domain Properties of the Correlation Channels	32
Simulations	36
Power Network Dynamics	40
Thermal Conductivity of Metals	45
The Multifrequency Method	51
Exercises	53
4. TREND ELIMINATION	56
Persson's Device	59
Exercises	63
5. SAMPLED SYSTEMS	64
Frequency Analysis	65
Finite Measurement Time	68
Diesel Engine Dynamics	70
Exercises	73
6. SUMMARY	75
7. ACKNOWLEDGEMENTS	76
8. NOTES AND REFERENCES	77
APPENDIX A - SIMULATION PROGRAMS	87
Jump Resonance	
A Frequency Analyser	
Effects of Random Disturbances	
Trend Elimination	

1. INTRODUCTION

Frequency response analysis is one of the oldest and most widely used methods to determine the dynamics of a stable linear system. When using the method the input signal is chosen as a sinusoid. If the system is stable the steady state the output signal is also a sinusoid with the same frequency as the input signal. A measurement of the amplitude and phase relations between the input signal and the steady state output signal then gives the value of the transfer function for $s = i\omega$ where ω is the frequency of the input signal. By repeating the measurement for different frequencies of the input signal the value of the transfer function can then be determined for any range of frequencies.

Frequency response analysis has been applied both in order to determine physical parameters and to determine dynamics for the purpose of control system design. The availability of the powerful frequency response method to determine the transfer function of a linear dynamical system was an important factor for the success of classical control theory.

A great advantage of the method is that the transfer function is obtained directly without extensive computation after the experiments. This means that various malfunctions and erroneous results can be detected very quickly. The experiments can then be repeated immediately without loss of time. Since the transfer function is obtained directly the method is also well suited to design techniques like the ones developed by Bode and Nichols which are explicitly based on the properties of the open loop transfer function. The equipment required for the experiment is very modest. It is necessary to have a sinewave generator and equipment to measure amplitude and phase relations between two sinusoids. For low frequencies the input signal can simply be introduced manually using a table and a clock.

It is also possible to use fairly crude approximations of a sinusoid. For higher frequencies a signal generator is, however, required. The amplitude and phase measurements can often be made from a recording of the inputs and the outputs on a two-channel recorder. Using a two-channel recorder it is also possible to detect nonlinearities as distortions in the output waveform and by comparing the results obtained with different amplitudes of the input signal. It is also possible to use an oscilloscope as a phase detector. Such simple schemes will work very well if there are small disturbances. For high disturbance levels the accuracy can be increased to an arbitrary degree at the price of longer experimentation time and slightly more sophisticated signal analysis equipment (correlators).

The main disadvantages of the frequency response method are the following:

- o The experiments may take a long time if low frequencies are considered.
- o The method permits determination of system dynamics only and cannot be used to model disturbances.

The chapter is organized as follows. A direct approach based on simple methods to determine amplitude and phase relations between two sine waves is discussed in Section 2. A more sophisticated technique based on correlation is discussed in Section 3. It is shown that disturbances can be rejected effectively at the price of increased experimentation time. A special method due to Jensen which reduces the experimentation time at the price of more computations is also briefly discussed. An efficient technique to eliminate the effects of drifting disturbances in the output are discussed in Section 4. Section 5 covers problems associated with frequency response analysis of sampled data systems.

To convey some feeling for the planning of experiments, the data analysis, and achievable results several practical examples based on real data are presented. The examples cover determination of dynamics of submarines, the human eye, a power network, a diesel engine, and determination of thermal diffusivity in metals.

Computer programs used to generate many of the figures in this chapter are included in the appendix. The programs include a flexible frequency analyser based on the correlation method. They are written in the interactive simulation language SIMNON.

2. A DIRECT APPROACH

Frequency response is based on the fact that for a stable linear system with the transfer function $G(s)$ the steady state response to the input

$$u(t) = u_0 \sin \omega t \quad (2.1)$$

is

$$y(t) = u_0 |G(i\omega)| \sin(\omega t + \arg G(i\omega)) \quad (2.2)$$

The value of the transfer function $G(s)$ for the argument $s = i\omega$ can thus be determined simply by applying a sinusoidal input to the system and comparing amplitudes and phases of the input and the output. By repeating this procedure for different values of the frequency ω the values of the transfer function can thus be determined for any desired range of frequencies.

To perform a frequency analysis a signal generator and equipment for comparison of amplitudes and phases of two sine waves are required. There are many different ways to make the comparison. The various schemes differ essentially in complexity and noise rejecting ability. A variable frequency sine wave generator and a recorder or an oscilloscope can be used as indicated in Fig. 2.1.

Signal generators with synchronized sine and square wave outputs are very common. They can be used for amplitude and phase measurements as shown in Fig. 2.3. It is even more convenient to use a sine wave generator with a variable phase output as shown in Fig. 2.2 although such generators are not as easily accessible.

The number of points ω_i required to obtain a sufficiently good approximation of the transfer function will, of

course, vary depending on the system and the application. A rule of thumb that is often given for typical servo-mechanism problems is to use about four points per decade. The points are frequently chosen as equally spaced on a logarithmic scale. This rule can, however, not be applied when the system has resonant peaks. Since there is no data processing involved the frequency curve is often plotted during the experiment. It is then easy to choose the frequencies ω_i on the basis of the results obtained.

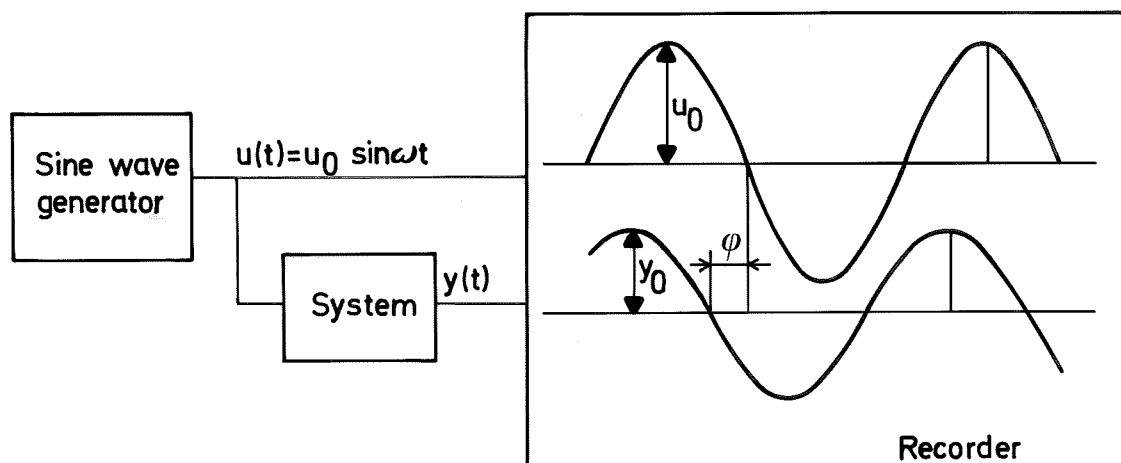


Fig. 2.1 - Experimental arrangement for the determination of the transfer function G of a stable linear system using a sine wave generator and a dual channel recorder or a dual beam oscilloscope. The magnitude of the transfer function is obtained as $|G(i\omega)| = y_0/u_0$ and the argument is given by $\arg G(i\omega) = \phi$. (Notice that ϕ is positive in the figure.)

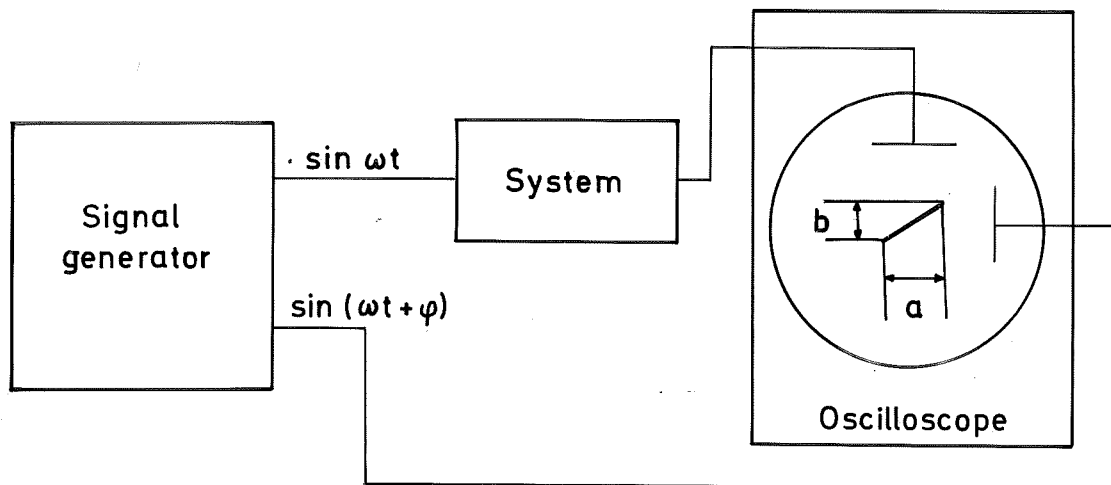


Fig. 2.2 - Experimental arrangement for the determination of the transfer function G of a stable linear system using a sine wave generator with variable phase shift and an oscilloscope. The variable phase is adjusted until the picture on the oscilloscope is a straight line. The phase shift then equals the argument $\arg G(i\omega)$ and the amplitude ratio is obtained as $|G(i\omega)| = b/a$. Notice that some care must be taken in order to avoid a phase error of π .

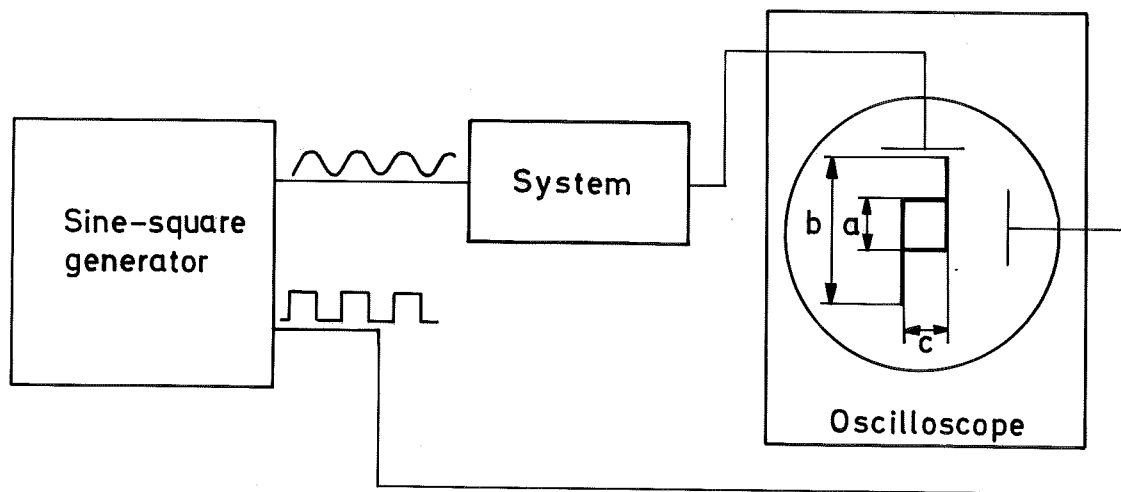


Fig. 2.3 - Experimental arrangement for the determination of the transfer function G of a stable linear system using a sine-square wave generator and an oscilloscope. The amplitude ratio is obtained by $|G(i\omega)| = \pi b/4c$ and the argument by $\arg G(i\omega) = \cos^{-1}(b/a)$. The zero crossings of the sine and square waves must coincide, and the signals must have the same peak-to-peak amplitude.

If there are considerable disturbances none of the arrangements shown in Figures 2.1, 2.2 or 2.3 will give satisfactory results. When there are disturbances the output of the system will contain not only the frequency of the input but other frequencies as well. A simple remedy is then to filter out the other frequencies. Before discussing this in detail some examples will be given.

Submarine Dynamics.

This application is based on experiments made in 1948 by Dr. A. Garde and Mr. E. Persson of the ASEA Company in collaboration with the Swedish Navy. The purpose of the experiments was to determine submarine dynamics for the purpose of designing a depth control system. It was thus of interest to know the dynamics relating depth to rudder angle. The application is of interest for several reasons. It shows that the input can be generated manually if the dynamics is sufficiently slow and that measurements can be performed with very simple equipment.

A schematic diagram of a submarine is shown in Fig. 2.4. The system to be analysed thus has one input, rudder angle β , and two outputs, pitch angle α and depth h . To determine the transfer functions, relating these variables, the rudder angle was varied sinusoidally. Since the frequencies of interest were very low, no signal generator was required. The sinusoidal variation was simply introduced manually according to a given program. The approximation of the sine wave used in the experiment is shown in Fig. 2.5. The pitch angle α and the depth h were read manually from a pendulum and a manometer.

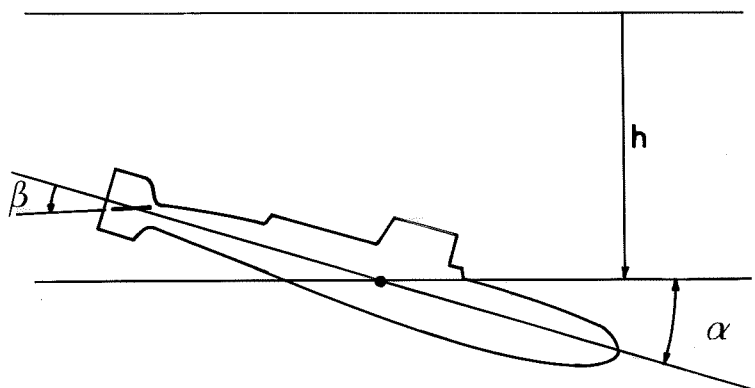


Fig. 2.4 - Pictorial diagram of a submarine. The rudder angle is β , the pitch angle α and the depth h .

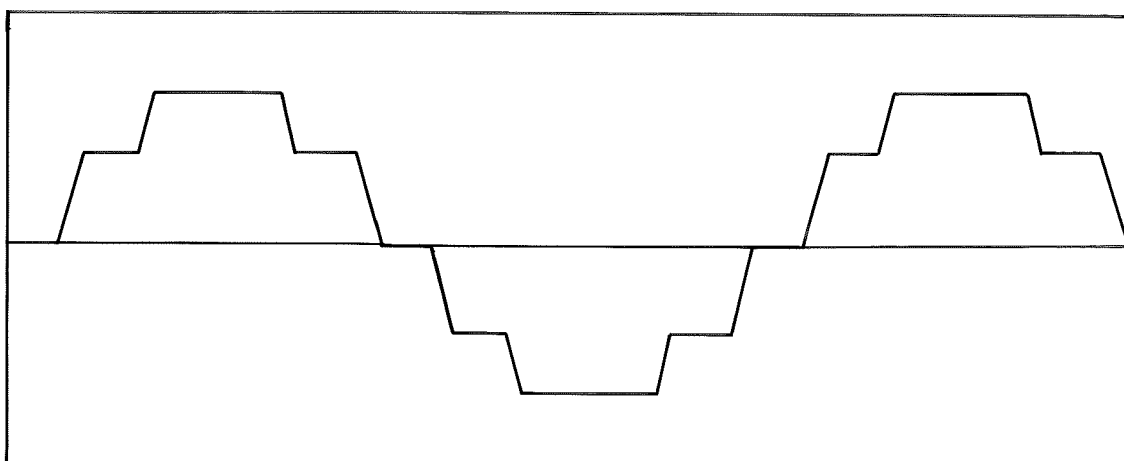


Fig. 2.5 - Approximation of sine wave used in experiment.

A typical result is shown in Figure 2.6. The amplitude ratio and the phase shift were determined directly from the graphs.

The experiment was repeated for different speeds. At high speeds the submarine was unstable and a low frequency oscillation of high amplitude was superimposed on the forced oscillation. See Fig. 2.7. The oscillation was partly due to instability and partly due to unsuccessful efforts to keep the depth within reasonable bounds through manual control of a rudder in the prow. The large variations in depth made the crew somewhat reluctant towards the benefits of automatic control. This attitude was changed drastically when the depth control system designed was finally put into operation. To determine the amplitude ratio in this case the low frequency variations were eliminated graphically as indicated in Fig. 2.7. Notice that this is a simple example of filtering.

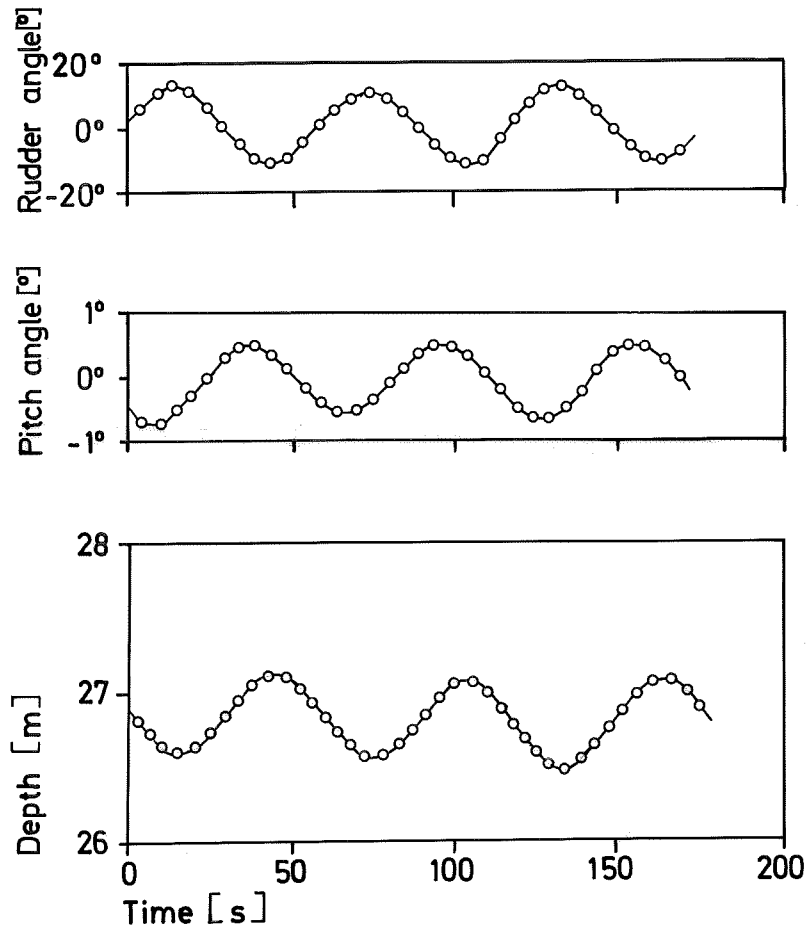


Fig. 2.6 - Input (rudder angle) and outputs (pitch angle and depth) obtained in the submarine experiment. The speed was 3 knots. (Redrawn from Garde Persson (1960)).

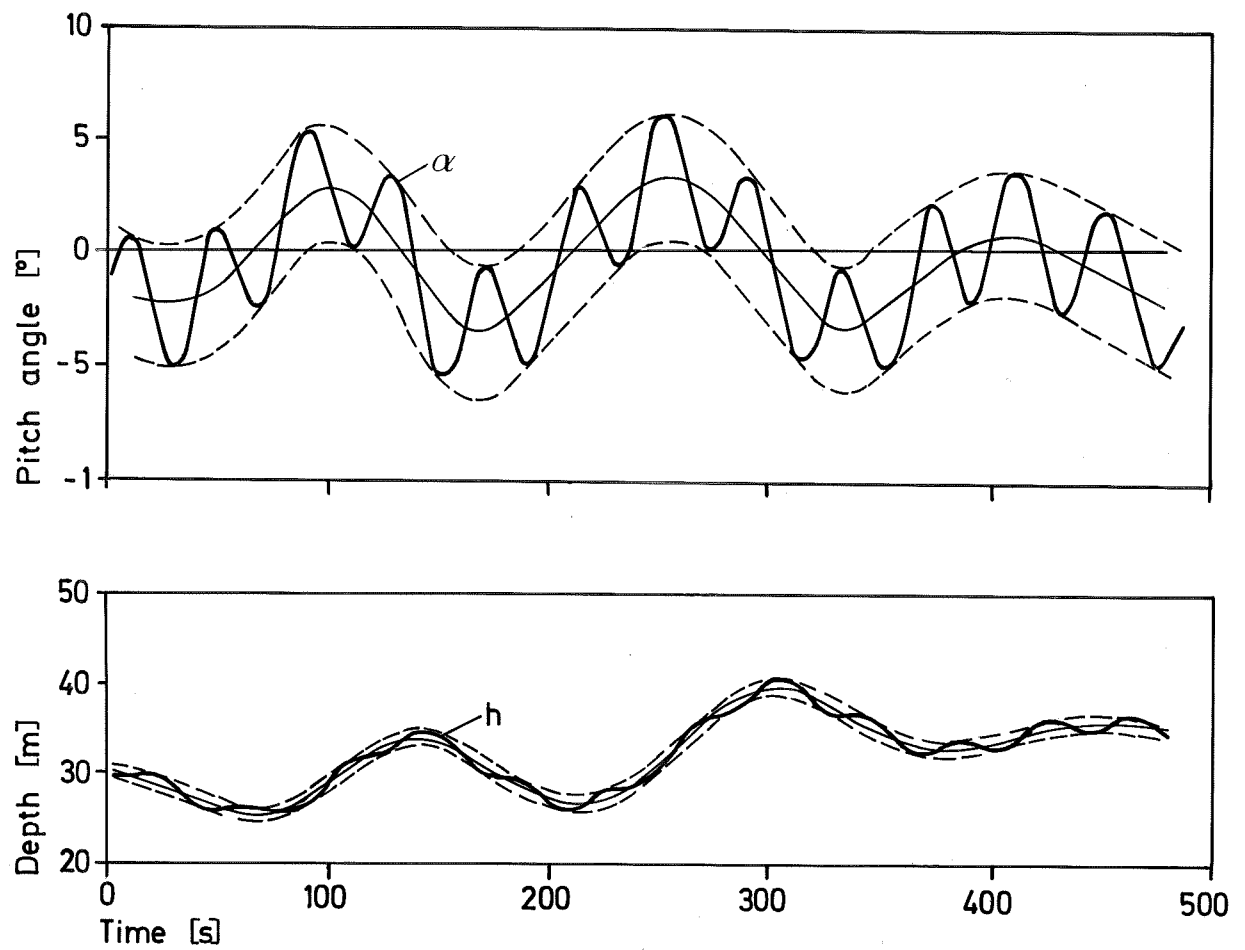


Fig. 2.7 - Pitch angle and depth obtained in submarine experiment at 7 knots. Notice that the variations, due to the input, are superimposed on a sinusoid of lower frequency and higher amplitude due to the instability of the submarine at high speeds. (Redrawn from material obtained from the Royal Swedish Navy).

Experiments were performed at three speeds 3, 5 and 7 knots. At each speed the value of the transfer function was determined at six values of the frequency using two different amplitudes of the input signal. The frequencies chosen correspond to periods of 30, 40, 60, 100, 150 and 200 s. The accuracy in the determination of the gain was about 10% and the error in the determination of the phase angle was about 10° . The results are summarized in the Bode diagrams in Figures 2.8 and 2.9. The results indicate that it seems reasonable to model the dynamics relating pitch angle to rudder angle as a linear system of at least second order. The results given in Fig. 2.8 clearly show that the dynamics is speed dependent. The damping in particular will decrease significantly with increasing speed.

As a complement to the frequency response analysis the steady state gain in the response of pitch angle was also measured statically.

A mathematical model of the submarine dynamics can be obtained from Newton's equations expressing the conservation of linear and angular momentum. Such an analysis leads to transfer functions of the form

$$\frac{L\{\theta\}}{L\{\delta\}} = \frac{b_1 s + b_2}{s^3 + a_1 s^2 + a_2 s + a_3}$$

$$\frac{L\{h\}}{L\{\delta\}} = \frac{c_1 s + c_2}{s[s^3 + a_1 s^2 + a_2 s + a_3]}$$

Transfer functions of this type can clearly be fitted to the data shown in Fig. 2.8 and Fig. 2.9.

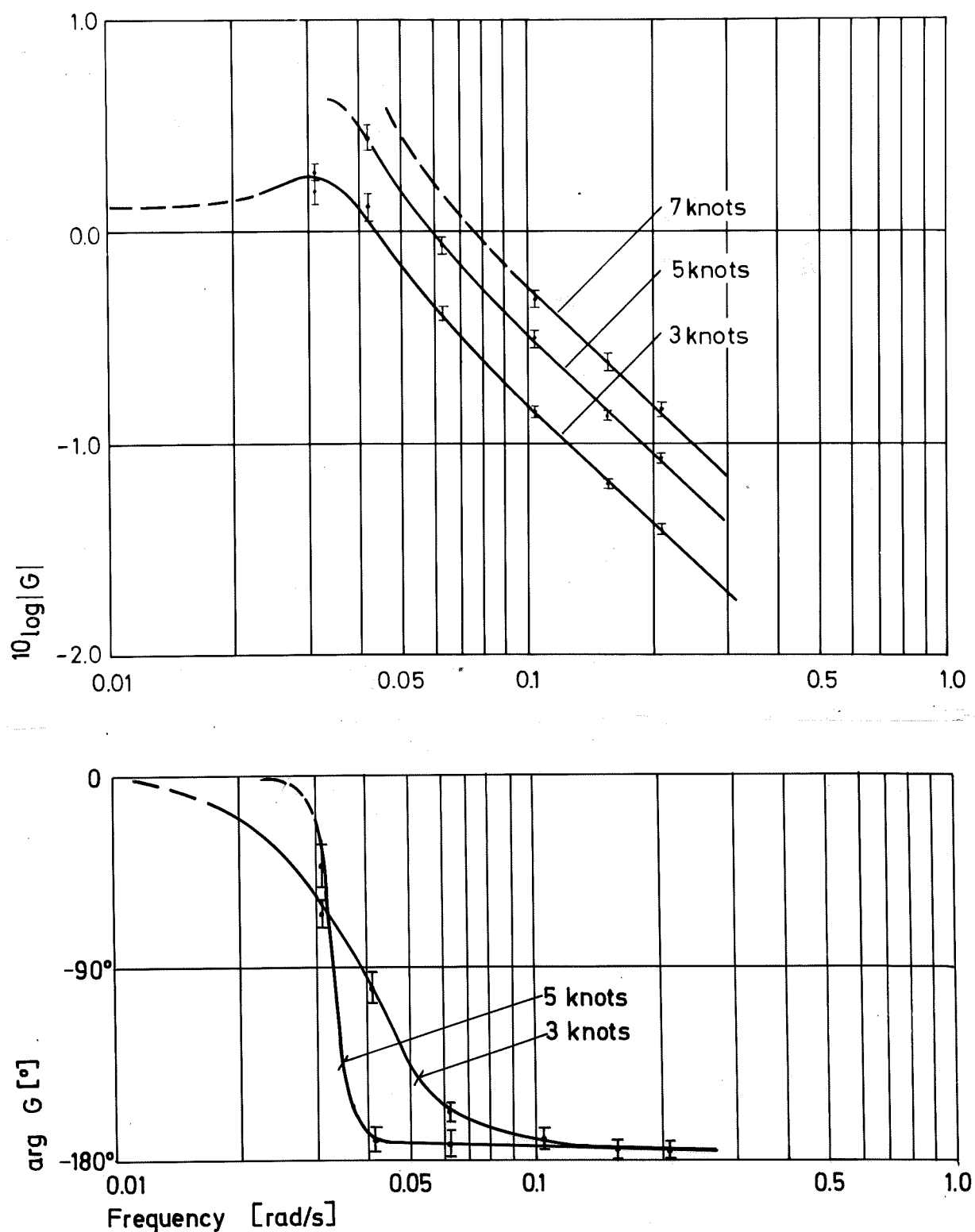


Fig. 2.8 - Bode diagram of the transfer function relating pitch angle to rudder angle obtained when applying frequency response to determine submarine dynamics. (Curves drawn from tables supplied by the Royal Swedish Navy).

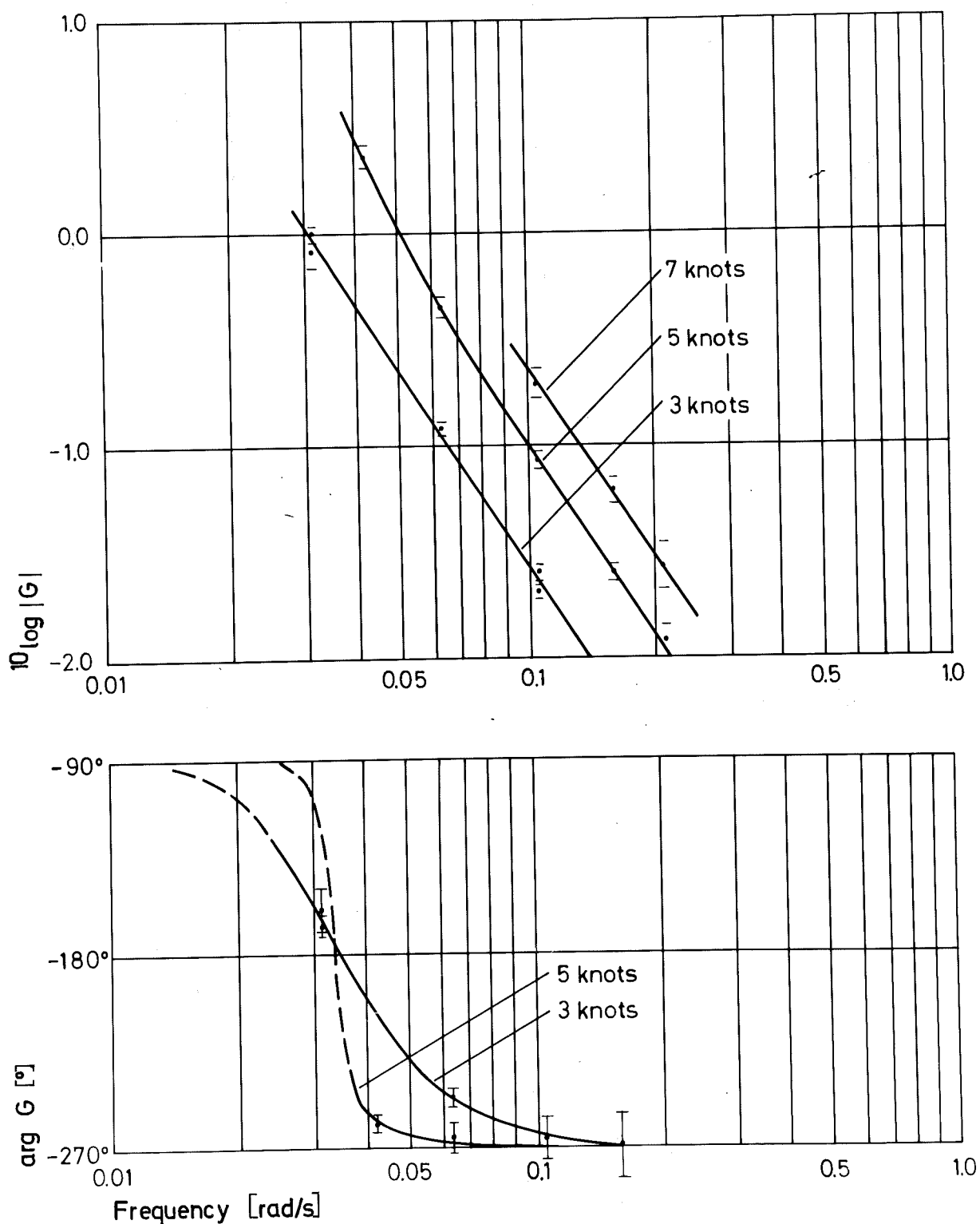


Fig. 2.9 - Bode diagram of the transfer function relating depth to rudder angle obtained when applying frequency response to determine submarine dynamics. (Curves drawn from tables supplied by the Royal Swedish Navy).

Pupillary Light Reflex Dynamics.

The second example is taken from physiology. It concerns the control system in the human eye which controls the size of the pupil in order to regulate the light intensity at the retina. The example is based on investigations by Stark (1959). The example is a good illustration of frequency response techniques and also a good illustration of clever experimental work. A block diagram of the control system is shown in Fig. 2.10. The area of the pupil is adjusted based on the light intensity at the retina to insure that this intensity is appropriate in spite of large and rapid changes in the light intensity outside the eye.

There is also another complex slow feedback which directly changes the sensitivity of the retina. This feedback accounts for the significant changes in sensitivity required for light and dark adaptation.

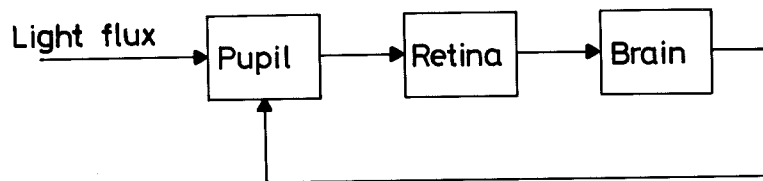


Fig. 2.10 - Block diagram of the control system which controls the pupil area in order to maintain the correct light intensity at the retina.

The area of the pupil can be determined optically by measuring reflection of infrared light. By stimulating the eye using an external light source and by measuring the area of the pupil it is possible to measure the closed loop response, i.e. the response in pupil area due to changes in the intensity of the external light source.

A fundamental property of feedback systems is that the closed loop response is usually fairly insensitive both to disturbances and to variations in the system parameters. The open loop system is often much more sensitive to parameter variations. Since one motivation for analysing physiological systems is to get insight into the physiological mechanisms it is thus of great interest to measure the open loop system. Such measurements are in general very difficult to perform on physiological systems because it is necessary to break the loop at a point, inject a signal and measure the signal which returns at the break point. Moreover, the signal transmission is often extremely complex, and it is difficult to find a suitable "break point".

In the particular case of the eye there is, however, a simple and elegant solution to the problem. The open loop response can be measured by varying the light intensity at the retina and measuring the size of the pupil. The retina can be stimulated directly by using a light beam which is so narrow that its cross section is smaller than the contracted iris. Hence by considering the pupil area as the output and the light intensity as the input both open loop and closed loop responses can be measured. The closed loop response is obtained when a broad light beam is used and the open loop response is obtained when a narrow beam is used. See Fig. 2.11.

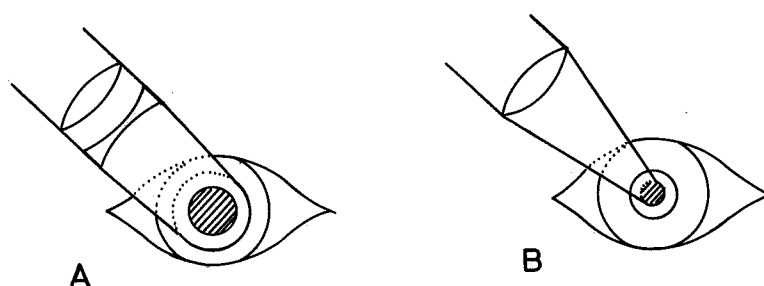


Fig. 2.11 - Illustration of the light stimulation method. Picture A shows the normal condition in which the variation in the iris changes the intensity at the retina. This gives the closed loop response. Picture B shows the technique used to obtain the open loop response. Due to the narrow beam the light intensity is not affected by the movement of the iris.

The following quotation from Stark (1959, p. 1930) explains why the frequency response method was chosen:

"There were three reasons for our use of sinusoidal stimuli: experimental techniques for obtaining given level of accuracy are simple, the mathematical analysis is well understood and relatively easy to manipulate, and system design and performance are evaluated readily. As an example of the first point, once the retina had adapted to mean light intensity, we were able to vary sinusoidal modulations over the entire frequency range while the pupil system remained in steady state."

Stark determined both the open loop and the closed loop transfer functions for the pupillary system using the techniques described above by varying the light source

intensity sinusoidally and measuring the pupil area. A sample of the measured inputs and outputs is shown in Fig. 2.12. A Bode plot of the open loop transfer function obtained is shown in Fig. 2.13. The individual measurements shown in Fig. 2.13 give an indication of the accuracy of the results.

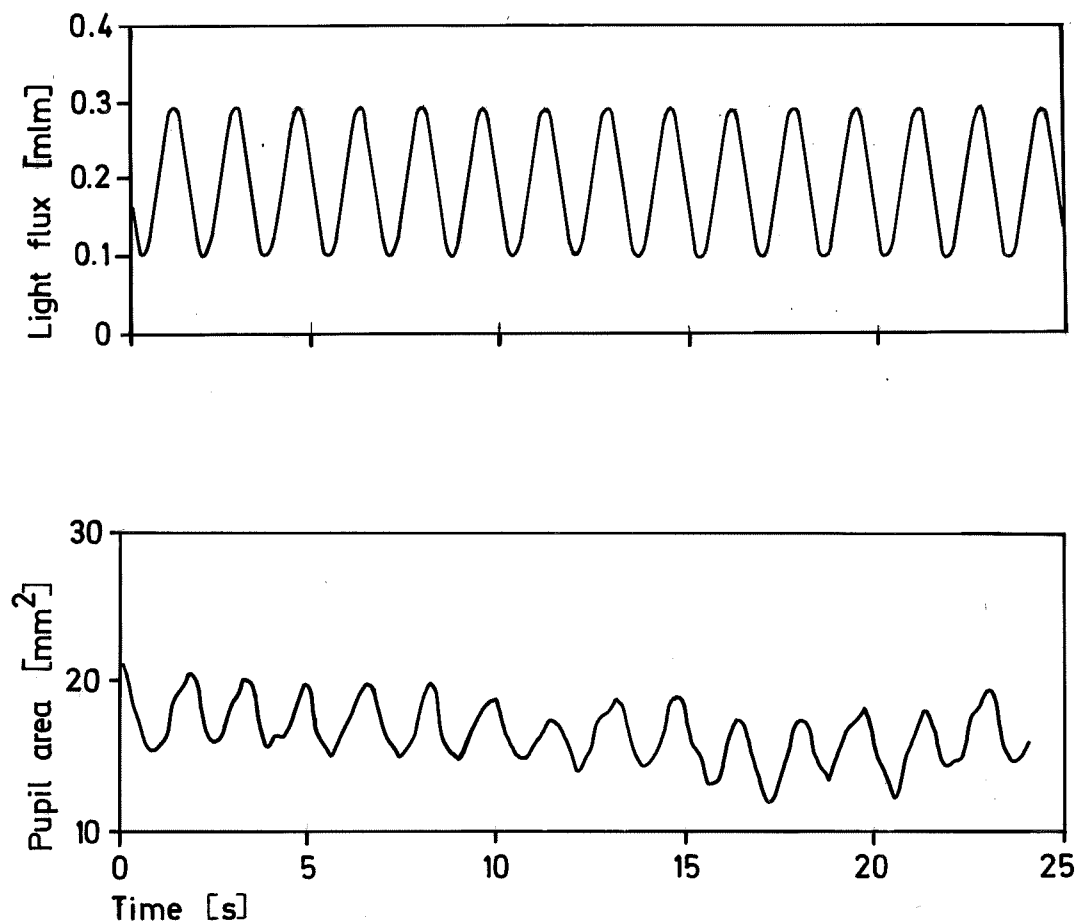


Fig. 2.12 - Input (light flux) and output pupil area obtained by an open loop experiment according to Fig. 2.11B. The curves are typical showing dominant fundamental response with harmonic distortion, high frequency noise and drift. The frequency of the input signal is 0.6 Hz. (Redrawn from Stark (1968))

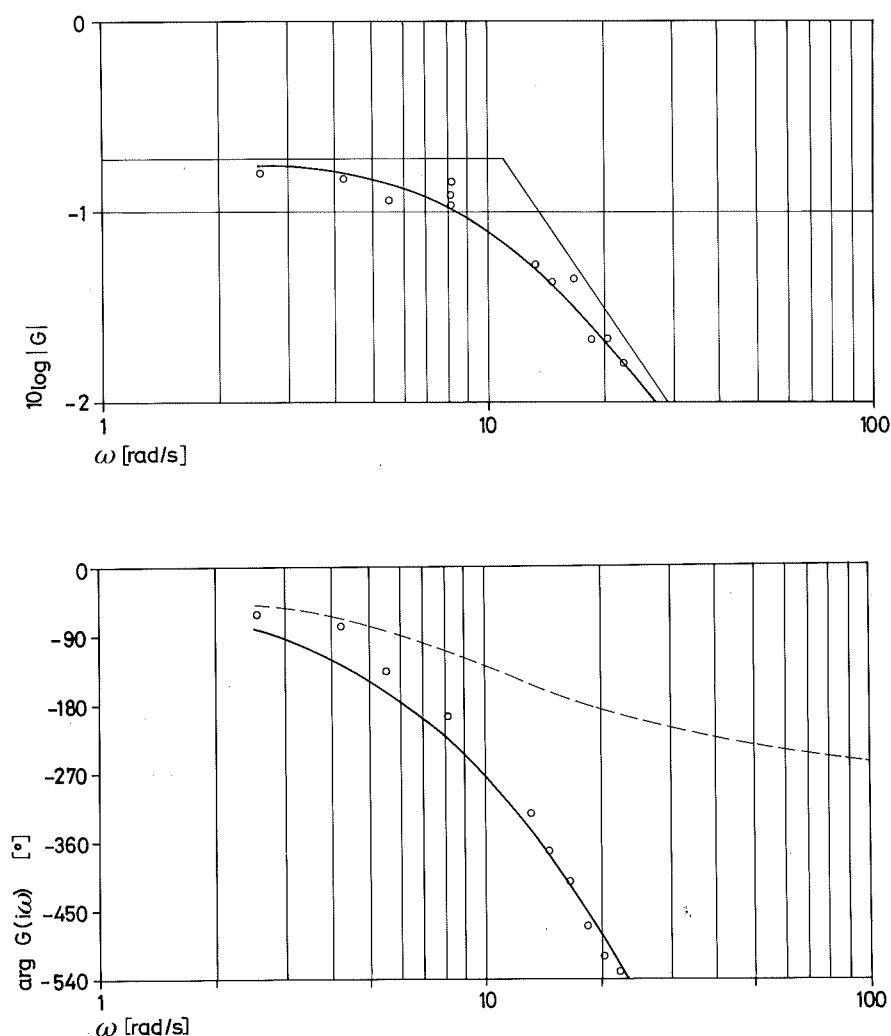


Fig. 2.13 - Results of the determination of the open loop transfer function relating pupil area to light flux. (Redrawn from Stark (1959))

To obtain an analytic approximation of the measured frequency response it is first observed that the amplitude ratio can be approximated by a rational transfer function of the form $G_1(s) = a/(1+sT_1)^3$. By crude graphical curve fitting it is found that the values $a = 0.19$ and $T_1 = 0.09s$ give a reasonable fit. The amplitude curve obtained is shown in Fig. 2.13. The corresponding phase curve is also indicated by the dashed line in the figure. Since the

dashed curve gives a very poor fit to the measured phase curve the difference between the dashed curve and the measurements is approximated by the transfer function $G_2(s) = \exp(-sT_2)$ which has unit gain. It is found that the value $T_2 = 0.18s$ is adequate. To summarize it is found that the measured points can be approximated by the transfer function

$$G_0(s) = G_1(s)G_2(s) = 0.19 \frac{1}{(1+0.09s)^3} e^{-0.18s} \quad (2.3)$$

This transfer function gives the relations between the normalized signals i.e.

$$\frac{\delta A}{A_0} = - G_0(s) \frac{\delta \Phi}{\Phi_0} \quad (2.4)$$

where A is the pupil area and Φ the light flux at the retina, δA denotes deviations in area and A_0 the reference value.

The frequency response method gives primarily the frequency curve which is a nonparametric representation on a linear system. It is sometimes of interest to have a parametric representation of the system dynamics. The method outlined above is a simple way to approximate a frequency curve by a rational function and a time delay. It is commonly used when high accuracy is not desired. Techniques to obtain parametric models are dealt with in depth in the following Chapters.

Unstable Systems.

The frequency response method cannot be applied to an unstable system if the experimental arrangement of Fig. 2.1 is used. The sinusoidal input will excite the unstable modes, the corresponding components of the output will then grow without bounds and totally dominate the component of the output which is due to the forcing input. Frequency response can, however, be used if the experimental conditions are changed by introducing a stabilizing compensator as shown in Fig. 2.14.

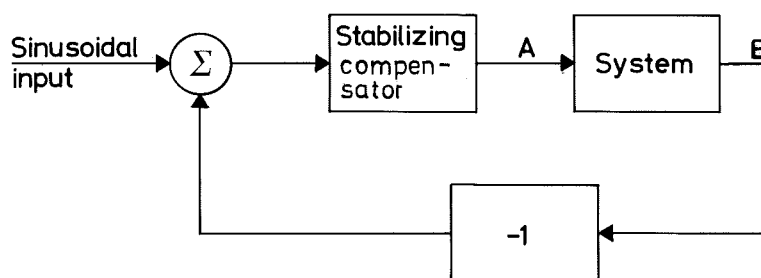


Fig. 2.14 - Experimental arrangement for frequency response of an unstable system. A stable closed loop system is obtained by introducing a stabilizing feedback. The reference value of the control loop is perturbed sinusoidally. The transfer function is measured by determining the amplitude and phase relations between the system input (A) and the system output (B).

Notice, that when a stabilizing feedback is used it is important that the reference input is perturbed. If this is

not done and if there are disturbances in the system, totally misleading results may be obtained as shown by the following example.

Example 2.1. Consider the closed loop system shown in Fig. 2.15. Assume that it is desired to determine the transfer function G_S by measuring the signals u and y .

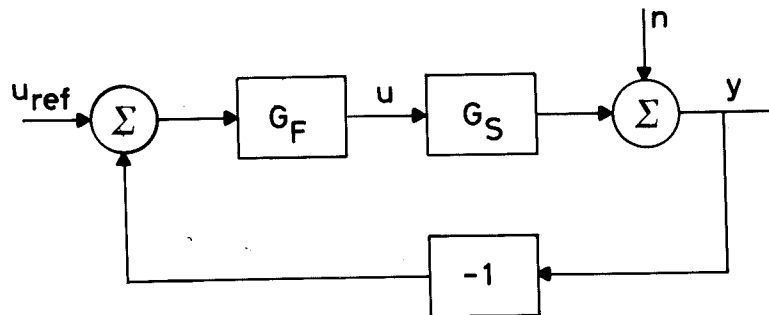


Fig. 2.15

Elementary calculations give

$$Y = \frac{G_S G_F}{1 + G_S G_F} U_{\text{ref}} + \frac{1}{1 + G_S G_F} N$$

$$U = \frac{G_F}{1 + G_S G_F} U_{\text{ref}} - \frac{G_F}{1 + G_S G_F} N$$

where U_{ref} , U , Y and N denote the Laplace transforms of u_{ref} , u , y and n . If the disturbance n is zero frequency response analysis gives the following transfer function

$$\hat{G} = \frac{Y}{U} = G_s$$

as could be expected. Notice, however, that if the reference signal u_{ref} is zero the following estimate of the transfer function is obtained

$$\hat{G}_s = \frac{Y}{U} = - \frac{1}{G_F}$$

The procedure will thus give the negative inverse of the transfer function of the stabilizing regulator, instead of the transfer function G_s of the system.

Nonlinear Systems.

The steady state response of a linear time-invariant dynamical system to a sinusoidal input is a sinusoid. It is thus possible to judge qualitatively if a system is linear and time-invariant by inspecting the output obtained from a frequency response test. Quantitative information can be obtained by using harmonic analysis or by determining the transfer function for different amplitudes of the input signal. Using the frequency response method it is thus possible to explore the signal amplitudes for which a linear time-invariant model is appropriate.

When performing a frequency response analysis of a nonlinear system several unexpected phenomena have been observed. For example it may happen that there are several equilibrium values of the amplitude of the steady state output. The servo system with a saturating amplifier shown in Fig. 2.16 has this property. This is illustrated in Fig. 2.17 which shows the outputs obtained when the system is

excited by a sinusoidal perturbation $u(t) = 0.5 \sin 1.3t$. The phenomenon which is also found in many other nonlinear systems is called jump resonance.

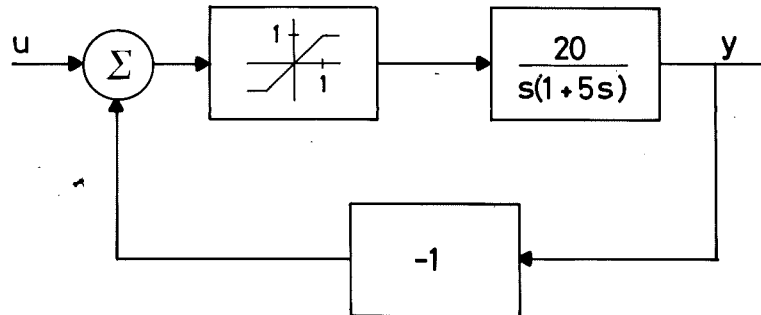


Fig. 2.16 - Block diagram of a servo system with a saturating amplifier.

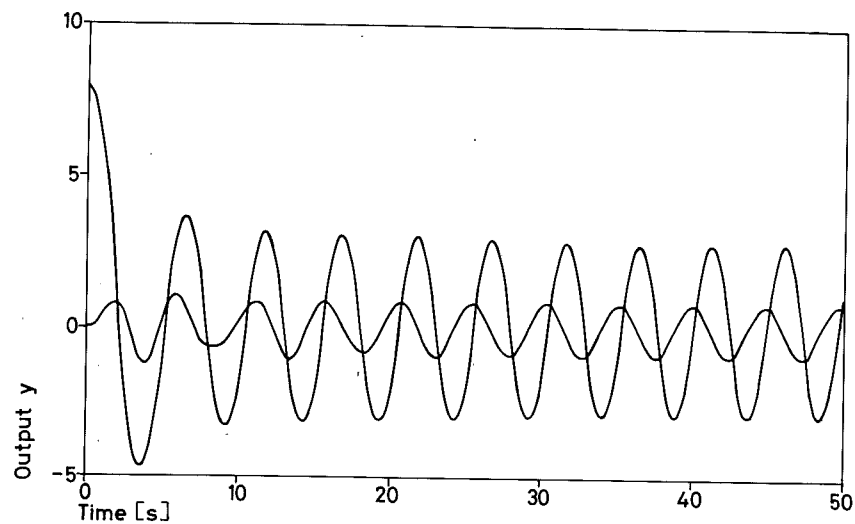


Fig. 2.17 - Outputs obtained when the reference input of the servo in Fig. 2.16 is $u(t) = 0.5 \sin 1.3t$. Notice that there are two possible steady state outputs.

Exercises.

1. A common, practical method for determining the phase angle and the amplitude is to estimate the phase angle by taking averages of several zero crossings and to estimate the amplitude by averaging either the extrema or the amplitudes midway between the zero crossings. Demonstrate that this procedure is reasonable by analysing the model

$$y(t) = a \sin(t+\varphi) + n(t)$$

where it is assumed that the density of the probability distribution of n is symmetric and that $n(t)$ and $n(t+\tau)$ are independent if $\tau \geq \pi/2$. The estimate of φ is given by

$$\hat{\varphi} = \frac{1}{N} \sum_{k=1}^N (t_k - \pi k - \pi)$$

where $\{t_k\}$ are the zero crossings. The estimates of the amplitude a are given by

$$\hat{a}_1 = \frac{1}{N} \sum_{k=1}^N |y(t_k + \pi/2)|$$

and

$$\hat{a}_2 = \frac{1}{N} \sum_{k=1}^N |y(t_i)|$$

where $\{t_i\}$ are the points where the signal has extrema. Show that the estimate $\hat{\varphi}$ is unbiased and that the estimates \hat{a}_1 and \hat{a}_2 have the properties

$$E \hat{a}_1 = a E \sqrt{1 - (\dot{n}(t)/a)^2}$$

$$E \hat{a}_2 = a E \sqrt{1 - (\dot{n}(t)/a)^2}$$

Notice that neither method will give good estimates if the disturbances are large. More efficient methods to handle large disturbances are discussed in the next section.

2. Consider the rudder angle and the depth curves shown in Fig. 2.6. Determine the magnitude and the phase angle of the transfer function.
3. Consider the pupillary light reflex dynamics according to Fig. 2.10. Let the light intensity be E , let the area of the light beam be a , the pupil area A and let the light flux be ϕ . For small perturbations the open loop response in pupil area to light flux is given by (2.4) where G_0 is the transfer function given by (2.3). Assume that the light beam is so wide that it covers the pupil completely. Show that the closed loop response is given by the transfer function

$$G = - \frac{G_0}{1 + G_0}$$

Determine the closed loop transfer function and particularly its low frequency gain. By direct measurement of the closed loop transfer function Stark found a low frequency gain of 0.15.

4. Consider the pupillary light reflex dynamics. The open loop gain can be increased artificially by using a narrow light beam which is focused on the edge of the pupil as shown in Fig. 2.18. Assume that the cross sec-

tions of the light beam and the pupil are circular and that the light beam is positioned as indicated in Fig. 2.19.

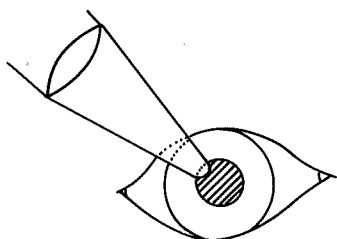


Fig. 2.18

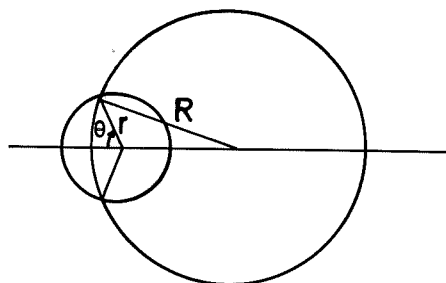


Fig. 2.19

Show that the closed loop response is given by the transfer function

$$\frac{\delta A}{\delta \phi} \cdot \frac{\phi_0}{A_0} = - \frac{G(s)}{1 + kG(s)}$$

where

$$k = \frac{R^2}{\pi r^2} \sin^{-1}(r/R \sin \phi)$$

Use the result to suggest an experiment which will give an unstable system. (This method was actually used by Stark as a verification of the open loop measurements.)

5. Simulate frequency response analysis of the servo mechanism with a saturating amplifier shown in Fig. 2.16 and verify the results of Fig. 2.17. Determine the frequencies for which there may be several amplitudes of the steady state output. What happens if it is attempted to determine the frequency response experimentally?

6. Demonstrate the possibility of performing frequency response of an unstable system by applying the scheme shown in Fig. 2.14 to determine the frequency response of a system described by

$$\frac{dy}{dt} = y + u$$

Simulate the results.

3. THE CORRELATION METHOD.

The method discussed in Section 2 is sensitive to disturbances because the amplitude ratio and the phase shift were evaluated in a primitive way using graphical methods. The accuracy of the determination of amplitude ratios and phase shifts in the presence of disturbances can be improved significantly by using correlation methods. A scheme which exploits this is shown in Fig. 3.1.

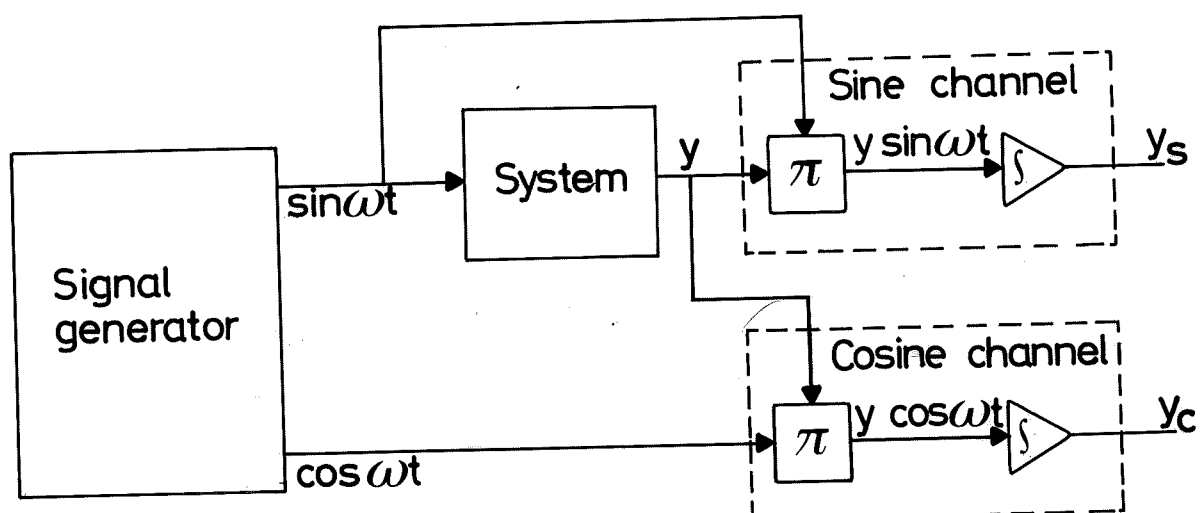


Fig. 3.1 - Frequency response analysis using an effective noise elimination scheme based on correlation of the output with sine and cosine functions.

The system is excited by a sine wave from the signal generator which also has a synchronized cosine output. The system output is multiplied by the sine and cosine signals and the products are integrated. The signal channels

are referred to as the sine channel and the cosine channel. The method requires a signal generator with synchronized sine and cosine signals, multipliers and integrators. Since the output of the multipliers is integrated, a bias in the multiplier output can lead to large errors. When using analog devices the analyser can be implemented using a servo multiplier, where the process output is applied to the servo potentiometer. It will be shown that the outputs of the sine and cosine channels are proportional to the real and imaginary parts of the transfer function.

Analysis.

The scheme for frequency response analysis shown in Fig. 3.1 will now be analysed. Let the input signal to the system be

$$u(t) = u_0 \sin \omega t \quad (3.1)$$

and let $y(t)$ denote the output of the system. If the system is stable and if the disturbances are neglected the steady state output is given by

$$y(t) = y_0 \sin(\omega t + \varphi) \quad (3.2)$$

where

$$y_0 = |G(i\omega)| u_0 \quad (3.3)$$

$$\varphi = \arg G(i\omega) \quad (3.4)$$

and G is the transfer function of the system.

The outputs y_s and y_c of the sine and cosine channels are given by

$$\begin{aligned}
 y_s(T) &= \int_0^T y(t) \sin \omega t \, dt = \int_0^T y_0 \sin \omega t \cdot \sin(\omega t + \varphi) \, dt = \\
 &= \frac{Ty_0}{2} \cos \varphi - \frac{y_0}{2} \int_0^T \cos(2\omega t + \varphi) \, dt
 \end{aligned} \tag{3.5}$$

$$\begin{aligned}
 y_c(T) &= \int_0^T y(t) \cos \omega t \, dt = \int_0^T y_0 \cos \omega t \cdot \sin(\omega t + \varphi) \, dt = \\
 &= \frac{Ty_0}{2} \sin \varphi + \frac{y_0}{2} \int_0^T \sin(2\omega t + \varphi) \, dt
 \end{aligned} \tag{3.6}$$

If the integration time is selected in such a way that ωT is a multiple of π we get

$$y_s(T) = \frac{1}{2} y_0 T \cos \varphi = \frac{T}{2} u_0 \operatorname{Re}\{G(i\omega)\}, \quad \omega T = \pi, 2\pi, \dots \tag{3.7}$$

$$y_c(T) = \frac{1}{2} y_0 T \sin \varphi = \frac{T}{2} u_0 \operatorname{Im}\{G(i\omega)\}, \quad \omega T = \pi, 2\pi, \dots \tag{3.8}$$

Hence if the integration time T is a multiple of π/ω the outputs of the integrators will be proportional to the real and imaginary parts of the transfer function. The scheme proposed thus appears to be a convenient scheme to determine the transfer function. Notice that a constant error in the measurement of the output will not influence the values of y_s and y_c for arguments which are multiples of $2\pi/\omega$.

Frequency Domain Properties of the Correlation Channels.

It will now be shown that the frequency analyser shown in Figure 3.1 has an excellent ability to reject disturbances. For this purpose it is convenient to give a frequency domain interpretation of the correlation channels. Consider for example the sine channel as a dynamical system with one input y and one output y_s . The input-output relation (3.5) is given by

$$y_s(t) = \int_0^t y(s) \sin \omega_0 s \, ds \quad (3.9)$$

This input-output relation represents a time-varying linear dynamical system and it has not a convenient frequency domain interpretation. Consider, however, the dynamical system characterized by the input-output relation

$$y_s(t) = \frac{1}{T} (-1)^{n-1} \int_{t-T}^t y(s) \sin \omega_0 (t-s) \, ds \quad (3.10)$$

Apart from the scaling factor $1/T$ which is introduced for convenience only the value of the output of (3.10) for $t = T$ will be the same as that of (3.9) if $\omega_0 T = n\pi$. For a fixed integration time T chosen as a multiple of π/ω_0 the sine channel of the correlator can thus be described by the linear time invariant system (3.10). This system will therefore be called the time invariant dynamical system associated with the sine channel. The frequency domain properties of (3.10) will now be investigated. The impulse response of the system is

$$h_s(t) = \begin{cases} \frac{1}{T} (-1)^{n-1} \sin \omega_0 t & 0 \leq t < T \\ 0 & t \geq T \end{cases} \quad (3.11)$$

Since $h_s(t) = 0$, for $t > T$, the filter has a finite settling time. To compute the transfer function of the filter (3.11) the transfer function G_1 of a filter with the weighting function

$$h_1(t) = \begin{cases} 1/T & 0 \leq t \leq T \\ 0 & t \geq T \end{cases} \quad (3.12)$$

will first be determined. The transfer function G_s is then obtained as the convolution of G_1 with the Laplace transform of $\sin \omega_0 t$. Observing that

$$\sin \omega_0 t = \frac{1}{2i} [e^{i\omega_0 t} - e^{-i\omega_0 t}]$$

and using the formula for translation in the s plane we get

$$G_s(s) = (-1)^{n-1} \frac{1}{2i} [G_1(s-i\omega_0) - G_1(s+i\omega_0)] \quad (3.13)$$

The transfer function G_1 is obtained simply by Laplace transforming h_1 . Hence

$$\begin{aligned} G_1(s) &= \int_0^{\infty} e^{-st} h_1(t) dt = \frac{1}{T} \int_0^T e^{-st} dt = \frac{1}{sT} [1 - e^{-sT}] \\ &= 2e^{-sT/2} \frac{\sinh sT/2}{sT} \end{aligned} \quad (3.14)$$

For $\omega_0 T = \pi, 2\pi, \dots$ the transfer function G_s associated with the sine channel of the correlator thus becomes

$$G_s(s) = \begin{cases} \frac{\omega_0}{(s^2 + \omega_0^2)^T} (1 + e^{-sT}) & \omega_0 T = \pi, 3\pi, \dots \\ -\frac{\omega_0}{(s^2 + \omega_0^2)^T} (1 - e^{-sT}) & \omega_0 T = 2\pi, 4\pi, \dots \end{cases}$$

A similar analysis of the cosine channel gives the following transfer function

$$G_c(s) = \begin{cases} -\frac{s}{(s^2 + \omega_0^2)^T} (1 + e^{-sT}) & \omega_0 T = \pi, 3\pi, \dots \\ \frac{s}{(s^2 + \omega_0^2)^T} (1 - e^{-sT}) & \omega_0 T = 2\pi, 4\pi, \dots \end{cases}$$

Fig. 3.2 and Fig. 3.3 show the amplitude curves of the transfer functions G_s and G_c . It is clear from these graphs that the correlation channels can be interpreted as bandpass filters with a center frequency ω_0 and a bandwidth proportional to $1/T$. The bandwidth can thus be made arbitrarily small by choosing sufficiently long integration time. The sine channel has a higher gain than the cosine channel for frequencies $\omega < \omega_0$ and a lower gain for frequencies $\omega > \omega_0$.

Let it finally be emphasized that the correlation channels are time-varying linear systems. The transfer functions (3.15) and (3.16) will describe the correlation channels only for integration times which are multiples of π/ω_0 . The transfer functions are useful to get an insight and to analyse the effect of disturbances on the correlator.

The filters with the transfer functions (3.15) and (3.16) have relatively high sidebands as is shown in Fig. 3.3. This is due to the discontinuities of the function h_1 of

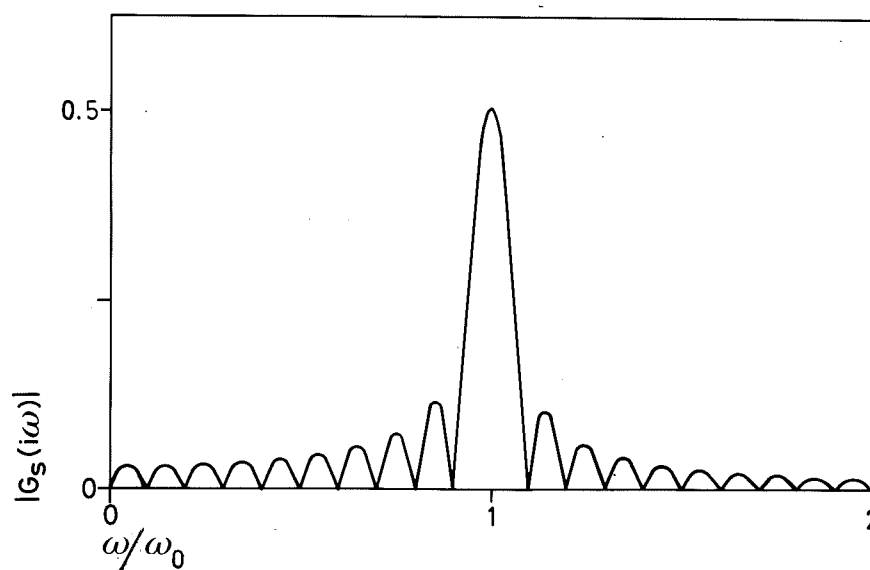


Fig. 3.2 - Amplitude curve for the transfer function G_s , given by the equation (3.15), which characterizes the sine channel of the frequency analyser. The curve is drawn for $\omega_0 T = 20\pi$.

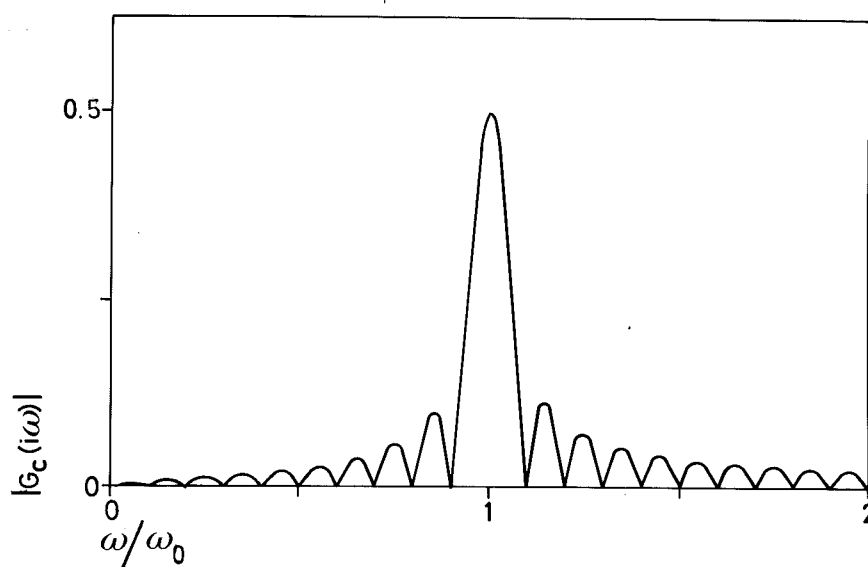


Fig. 3.3 - Amplitude curve for the transfer function G_c , given by the equation (3.16), which characterizes the cosine channel of the frequency analyser. The curve is drawn for $\omega_0 T = 20\pi$.

(3.12). The sidebands can be reduced if the function h_1 is replaced by a smooth function for example

$$h_1(t) = \begin{cases} (1 - \cos 2\pi t/T)/T & 0 \leq t \leq T \\ 0 & t > T \end{cases} \quad (3.17)$$

This is often referred to as a time window. The scheme can be implemented by multiplying the sine and cosine signals from the signal generator by the function $1 - \cos 2\pi t/T$ before they are multiplied by the output $y(t)$.

Simulations.

Some properties of the correlation method will now be illustrated by simulations. For this purpose a system with the transfer function

$$G(s) = \frac{1}{1 + s}$$

is considered. The input is chosen as a sinusoid with unit amplitude and the frequency 1 rad/s. For this frequency the amplitude ratio of the transfer function is $1/\sqrt{2}$ and the phase angle is $-\pi/4$ or -45° . Fig. 3.4 shows the input u , the output y , the integrator outputs y_s and y_c and the estimates of the magnitude and the phase angle of the transfer function.

The possibilities to use the correlation method when there are large disturbances are illustrated in the simulations shown in Fig. 3.5. Results are shown for the noise free case (A) and when disturbances are added to the system

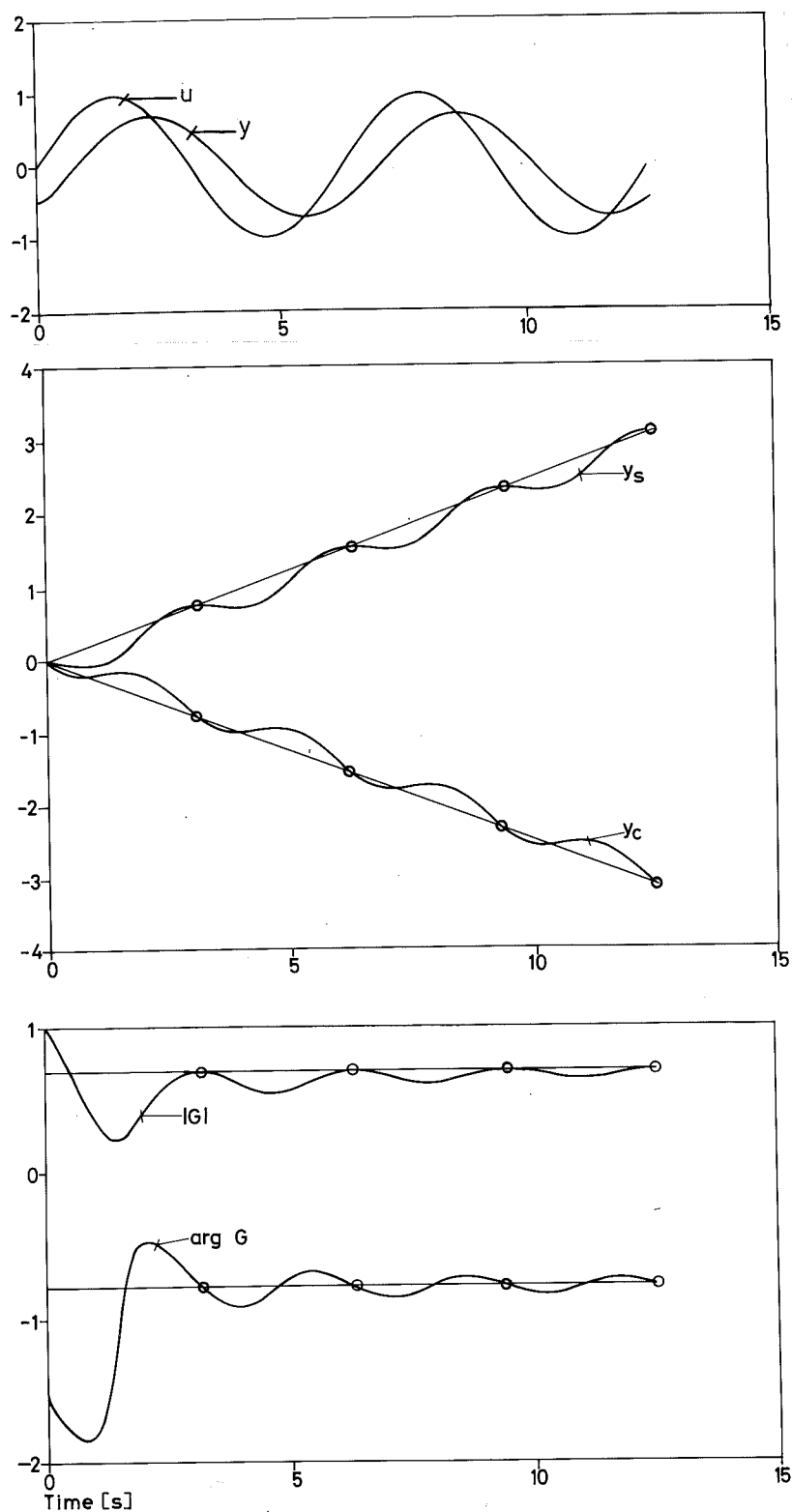


Fig. 3.4 - Results of simulation of frequency analyser based on the correlation method. The graphs show the system input u , the system output y , the outputs of the correlation channels and the estimated magnitude and phase angle of the transfer function. Notice that the estimate of the transfer function can be expected to be correct only for $t = \pi, 2\pi, 3\pi, 4\pi$.

output. The disturbance was generated by feeding white noise through first order filters with time constants 0.1 s and 10 s in cases B and C respectively. The signal to noise ratio was one in both cases. The integration time T was five periods.

The simulations show clearly that a frequency analyser based on the correlation method has excellent noise rejecting properties.

The estimates obtained are given in Table 3.1.

Table 3.1 - Estimates of the transfer function obtained from the experiments in Fig. 3.5.

Case	abs G	arg G
A	0.707	-0.754
B	0.702	-0.792
C	0.714	-0.695
true	0.707	-0.785

The deviation from the true values in case A depends on the fact that the system was not in steady state when the measurement was started. The deviations in the other cases are also due to the disturbances. Notice that it is possible to determine the magnitude with an accuracy of about 1% in spite of the large disturbances. The error in the phase angle is 1% in case B and 10% in case C. Also notice that the error in the phase angle due to non-stationarity is very significant 4%. It is thus important to make sure that the system is in a steady state before the measurement is started.

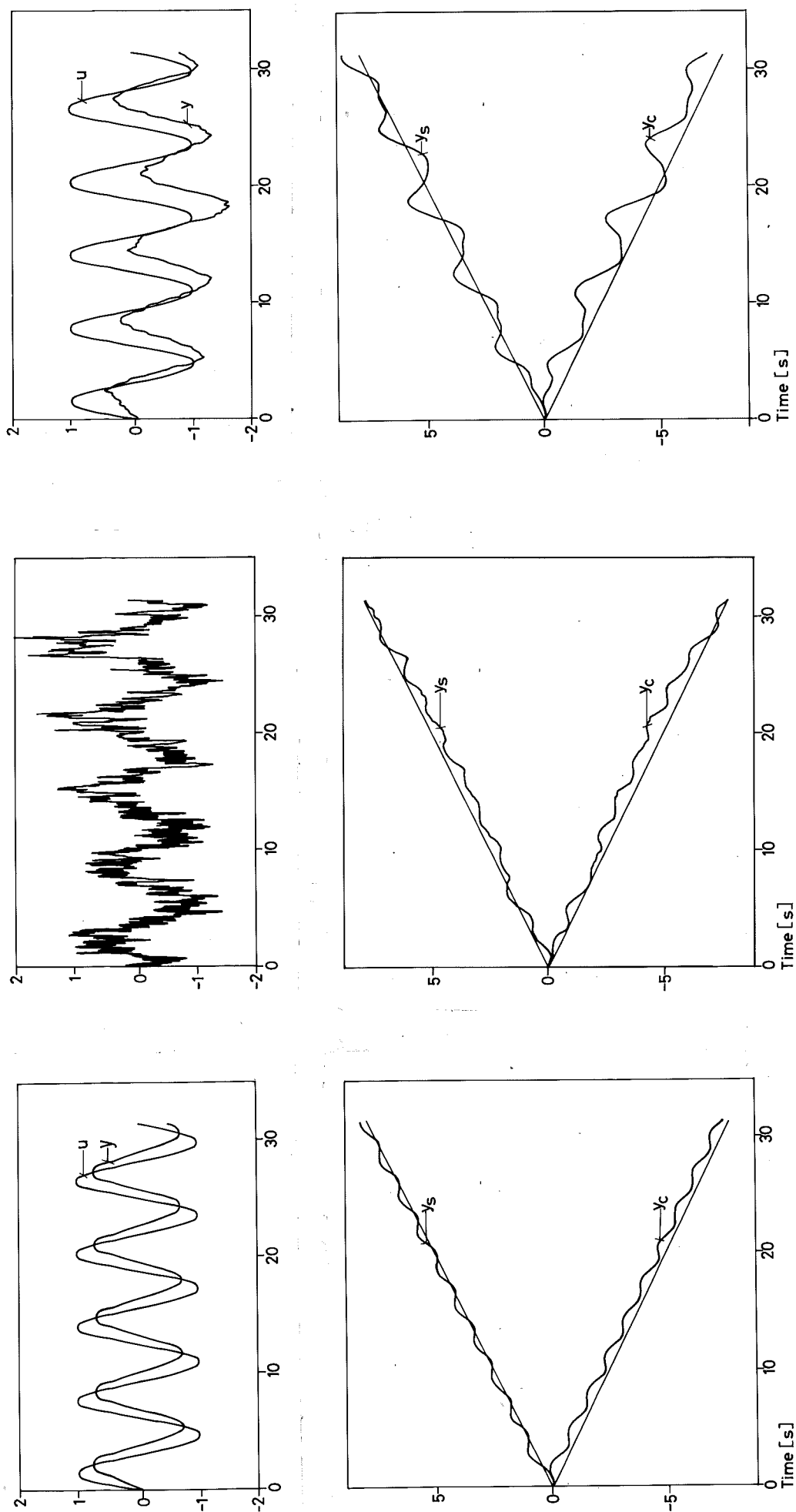


Fig. 3.5 - Results of simulation of frequency analyser based on correlation.
The system and the input are the same as in Fig. 3.4.

Power Network Dynamics.

When designing control systems for electric power stations it is important to know how the network frequency is influenced by the power generated in one station. A crude estimate of the dynamics involved can be obtained from an energy balance for the whole power network. Let E denote the total stored energy, P_g the generated power, P_c the consumed power and P_ℓ the power loss. An energy balance for the whole power network then gives

$$\frac{dE}{dt} = P_g - P_c - P_\ell \quad (3.18)$$

The major part of the energy is stored in terms of kinetic energy of rotating machines. If it is assumed that all rotors are in synchronism their angular velocities ω are identical and proportional to the frequency f of the network. The total stored energy can then be expressed as

$$E = \frac{1}{2} J \omega^2 = k f^2$$

where J is the sum of the moments of inertia of all rotors. The consumed power P_c also depends on the frequency.

Introducing the above expression for E into (3.17) and linearizing the resulting equation, it is found that for small deviations the relation between the frequency f and the generating power can be expressed by the transfer function

$$\frac{L\{\delta f\}}{L\{\delta P_c\}} = \frac{K}{1 + sT} \quad (3.19)$$

where

$$K = 1/P'_C(f_0)$$

$$T = E'(f_0)/P'_C(f_0)$$

The model (3.19) will hold only for slow variations in the generated power. For rapid variations in generated power the rotors of the different machines will no longer be in exact synchronism. There will also be energy stored in transformers and power lines. To describe the system in such cases it is then necessary to make a much more detailed model. The dynamics will also depend on where the power is injected and where the frequency is measured. The transfer function (3.19) for the Swedish power network was measured by Garde, Oja and Persson of the ASEA Company in collaboration with the Swedish Power Board in 1949.

In the experiments the governors of all turbines were locked firmly and the frequency was held by manual regulation. The output of one 50 MW machine at the Midskog power station was varied sinusoidally at different frequencies in the range 0.05 - 1.0 rad/s. The resulting variations in the net frequency were measured. The amplitude of the power fluctuations was about 10 MW. The total generating capacity of the system was about 2200 MW.

Fig. 3.6 shows the normal fluctuations in frequency as well as the fluctuations, observed when test signals were introduced in the system. As is clearly seen from Fig. 3.6 the normal fluctuations are much larger than the fluctuations generated by the perturbations. For the frequencies $\omega = 0.105$ rad/s, $\omega = 0.22$ rad/s,

and $\omega = 0.42$ rad/s the effect of the input is clearly visible in the graphs. At the higher frequencies $\omega = 0.84$ rad/s and $\omega = 1.05$ rad/s the effect of the input is hardly noticeable in the output. It is thus not possible to determine the transfer function of the power system by a direct comparison of amplitude ratios and phase shifts for the input and the output. Using the correlation method it is, however, possible to obtain good results even for the data shown in Fig. 3.6 for $\omega = 1.05$.

In the particular case the necessary multiplication was done with a watt-meter and the integration was done by a ballistic galvanometer¹⁾ whose deflection was read manually. To overcome the problem of finite scale the polarity of the signal was reversed when the meter deflection reached the limit. Fig. 3.7 shows the outputs of the sine and cosine channels for measurements at $\omega = 0.42$ rad/s. In Fig. 3.8 are shown the Nyquist curves obtained from the experiments. The results show that a linear model relating frequency changes to power input can be described by the transfer function (3.19) where the gain K and the time constant depend on the operating conditions. Typical values are given below.

	T[sec.]	K[hz/MW]
Weekday 13 - 15	7.2	0.0084
Weekday night	7.7	0.013
Sunday afternoon	5.9	0.017

1) A ballistic galvanometer is a galvanometer without spring restraint. Its transfer function is approximately given by $K/(s^2 + Ds)$.

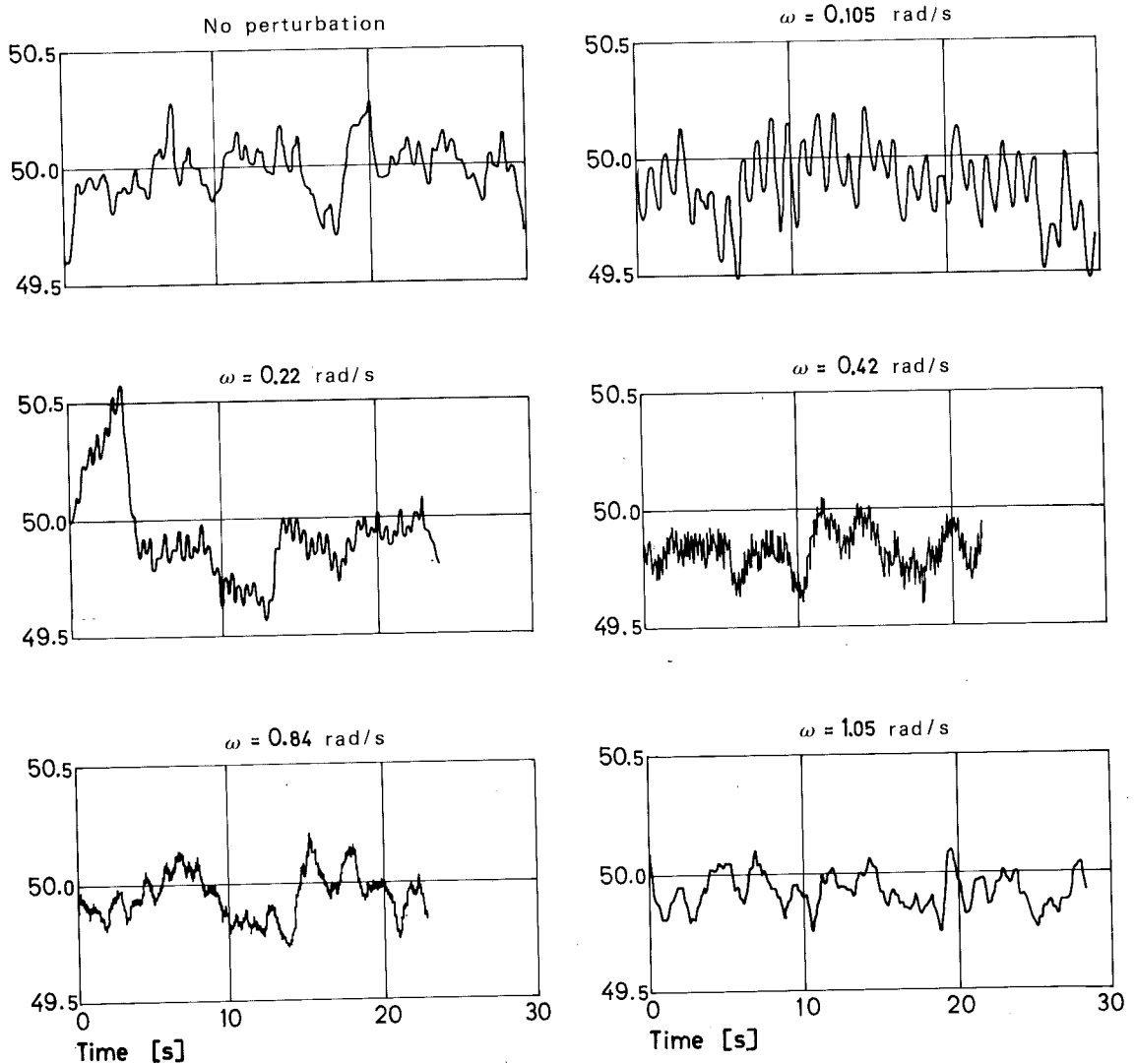


Fig. 3.6 - Measurements of fluctuations in frequency of the Swedish power net during normal conditions and when sinusoidal power perturbations of different frequencies are injected. The ordinate is the net frequency [Hz] in all graphs. (Redrawn from Persson (1967)).

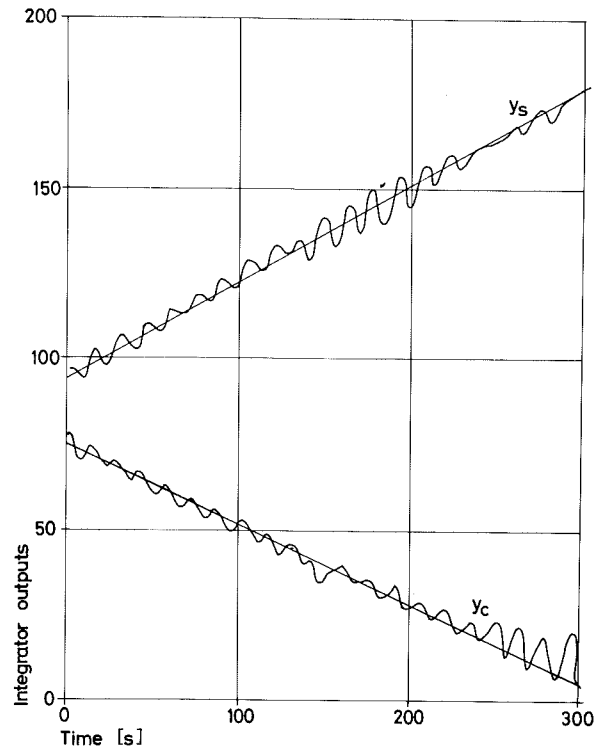


Fig. 3.7 - Outputs of the sine and cosine channels when measuring the frequency response of the Swedish power net at a frequency of 0.42 rad/sec. (Redrawn from Almström and Garde (1950)).

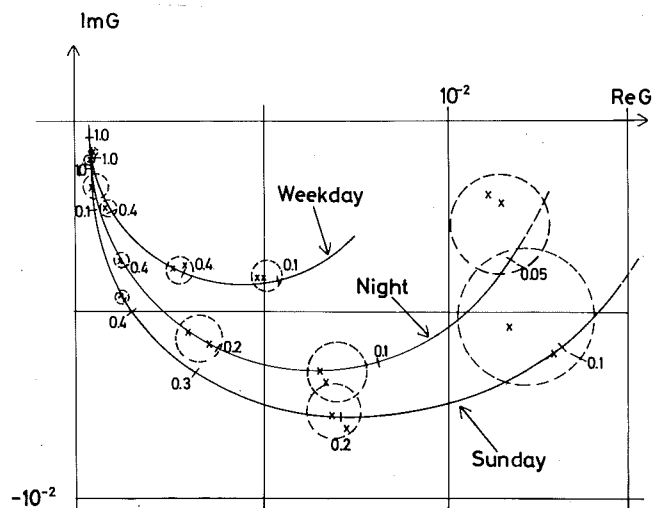


Fig. 3.8 - Nyquist diagram of a linear model of the Swedish power net obtained from the ASEA measurements. The circles indicate measurement uncertainty. (Redrawn from Almström and Garde (1950)).

Thermal Conductivity of Metals.

A very neat application of frequency response analysis was published in 1861 by the Swedish physicist Ångström, who used the method to determine thermal conductivity of metals. A simplified diagram of Ångström's apparatus is shown in Fig. 3.9. The basic idea is to take a long metal rod with a small cross section. By periodically varying the temperature at one end point, a heat-wave is generated. The thermal diffusivity is then determined by analysing the attenuation and phase shift of the heat wave as it progresses down the rod.

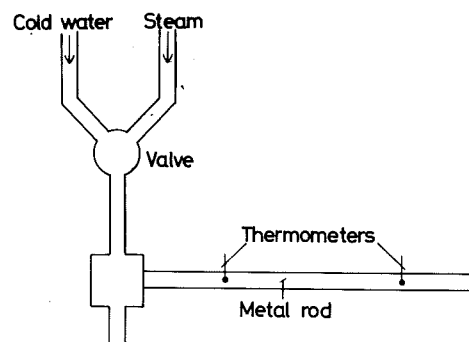


Fig. 3.9 - Simplified diagram of the apparatus used by Ångström to determine thermal diffusivity of metals. In the original experiment the copper rod had a length of 570 mm and a diameter of 23.75 mm. Several holes of diameter 2.25 mm for thermometers were drilled at positions of 50 mm apart.

To carry out the analysis it is assumed that the system can be described as a semi-infinite rod with small heat losses to a medium of constant temperature. The rod can then be described by the one-dimensional heat equation

$$\frac{\partial u}{\partial t} = \kappa \frac{\partial^2 u}{\partial x^2} - \mu u \quad (3.20)$$

where $u(t,x)$ denotes the temperature at time t at a point along the rod with coordinate x . The parameter κ is the thermal diffusivity defined by

$$\kappa = \frac{\lambda}{\rho c} \quad (3.21)$$

where λ is thermal conductivity, c specific heat, and ρ density. The term μu in equation (3.20) represents any heat loss to the environment due to radiation, conduction, or convection. Since the heat losses in general are nonlinear functions, the approximation by a linear term is valid for small deviations only. The value of the parameter μ will then also depend on the chosen operating condition.

The mathematical model (3.20) contains two parameters, κ and μ , and the problem is to determine the thermal diffusivity κ .

By taking Laplace transforms, it is easily shown that the transfer function relating the temperature at coordinate x to the end point temperature is given by

$$G(s) = \frac{U(s,x)}{U(s,0)} = \exp(-x \sqrt{(s+\mu)/\kappa}) \quad (3.22)$$

Also notice that this function can be interpreted as the transfer function which relates temperatures at two arbitrary points on the rod with spacing x .

Straightforward calculations give

$$\log |G(i\omega)| = -x \sqrt{(\omega^2 + \mu^2) / (2\kappa)}$$

$$\arg G(i\omega) = -x \sqrt{(\omega^2 + \mu^2) / (2\kappa)}$$

Multiplication now gives the equation

$$\log |G(i\omega)| \cdot \arg G(i\omega) = \frac{x^2 \omega}{2\kappa} \quad (3.23)$$

which according to Ångström is "ein durch seine Einfachheit merkwürdiges Resultat". By measuring the value of the transfer function at one particular frequency ω , the thermal diffusivity can thus easily be determined by Ångström's formula (3.23). Apart from the discovery of equation (3.23), there are several interesting features of Ångström's experiment. The heat-wave was generated manually by changing a valve which either admits steam or cold water to the small chamber at the end of the rod. It follows from the transfer function (3.22) that higher harmonics are significantly damped, which means that the signals will resemble sine-waves at some distance from the end point. See Fig. 3.10.

The periods chosen in the experiment were 12, 16 and 24 minutes. The spacings between the thermometers were selected as 50 mm, 100 mm, and 150 mm.

It is clear from Fig. 3.10 that the temperatures are not well approximated by sinusoids. To remove the remaining harmonics a trigonometric polynomial was fitted to the data. This is mathematically equivalent to using a correlation technique as was described in the beginning of this section. For the data shown in Fig. 3.10 the following result was obtained.

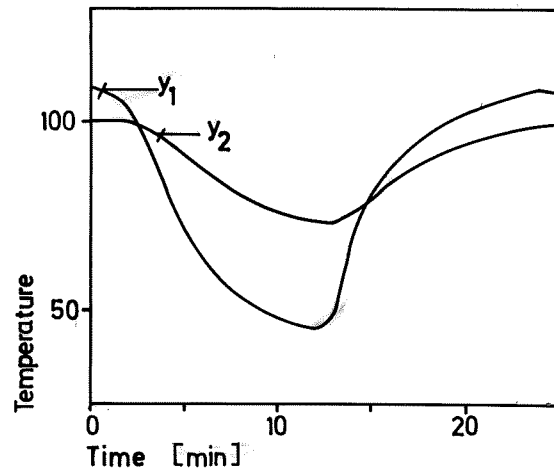


Fig. 3.10 - Results of Ångström's experiment. The curves are temperatures of a copper rod at points spaced 0.1m. The end point temperature is varied periodically with a period of 24 min.

$$\begin{aligned}
 y_1^1(t) &= 80.39 + 31.745 \sin(15t+134.10^\circ) + \\
 &\quad + 4.578 \sin(30t+14.53^\circ) + 3.717 \sin(45t+104.55^\circ) \\
 y_2^1(t) &= 88.86 + 13.010 \sin(15t+109.04^\circ) + \\
 &\quad + 1.591 \sin(30t+337.26^\circ) + 1.187 \sin(45t+61.97^\circ) \quad (3.24)
 \end{aligned}$$

The time unit is minutes.

To eliminate in the thermometer scale factors Ångström simply repeated the experiment with the thermometers interchanged. For this case he obtained the following trigonometric series:

$$\begin{aligned}
y_1^2(t) &= 74.57 + 25.203 \sin(15t+142.35^\circ) + \\
&\quad + 2.186 \sin(30t+54.48^\circ) + 4.334 \sin(45t+112.42^\circ) \\
y_2^2(t) &= 82.93 + 23.885 \sin(15t+117.79^\circ) + \\
&\quad + 1.665 \sin(30t+18.46^\circ) + 2.969 \sin(45t+70.68^\circ) \quad (3.25)
\end{aligned}$$

Let the scale factors of the thermometers be α_1 and α_2 and let the true temperatures be y_1 and y_2 . The first measurement gives

$$y_1^1 = \alpha_1 y_1$$

$$y_2^1 = \alpha_2 y_2$$

and the measurement with the thermometers reversed gives

$$y_1^2 = \alpha_2 y_1$$

$$y_2^2 = \alpha_1 y_2$$

Elimination of the calibration factors α_1 and α_2 gives

$$\frac{y_2}{y_1} = \sqrt{\frac{y_2^1}{y_1^1} \cdot \frac{y_2^2}{y_1^2}}$$

The magnitude of the transfer function is thus given by

$$|G(i\omega)| = \sqrt{\frac{13.010 \cdot 23.885}{31.745 \cdot 25.203}} = 0.6232$$

and its argument is given by

$$\arg G(i\omega) = -24.8^\circ = -0.433 \text{ rad}$$

Since $\omega = 2\pi/(24.60)$ and $x = 0.1$, equation (3.22) gives

$$\begin{aligned} \kappa &= \frac{x^2 \omega}{2 \log |G(i\omega)| \arg G(i\omega)} = \frac{10^{-2} \cdot 2\pi}{2 \cdot 0.473 \cdot 0.433 \cdot 24.60} = \\ &= 1.07 \cdot 10^{-4} \text{ [m}^2/\text{s]} \end{aligned}$$

This value agrees favourably with $\kappa = 1.18 \cdot 10^{-4} \text{ m}^2/\text{s}$ (100°C) given in Goldsmith (1961, 247-266).

To obtain a value for the thermal conductivity λ , Ångström used equation (3.21) and available values for the density ρ and the specific heat c . Through his method Ångström could improve the determination of thermal conductivity significantly. Earlier values obtained by Péclet were $79\text{W/m}\cdot\text{K}$ for copper and $30\text{W/m}\cdot\text{K}$ for iron. Ångström obtained the values $382\text{W/m}\cdot\text{K}$ for copper and $68\text{W/m}\cdot\text{K}$ for iron which are very close to values found in modern tables. By applying frequency response analysis Ångström was thus able to make a significant improvement in the determination of thermal diffusivity.

The Multifrequency Method.

One disadvantage of the frequency response method is that the experiments may take considerable time since the measurements have to be repeated for each frequency. A modification by Jensen (1959) eliminates this drawback at the price of increased complexity in the data analysis. The basic idea is simple. The time is reduced by introducing several sinusoids simultaneously. Jensen starts with the signal

$$u(t) = \cos \omega t - \cos 2\omega t + \cos 4\omega t - \cos 8\omega t + \\ + \cos 16\omega t - \cos 32\omega t + \cos 64\omega t \quad (3.26)$$

which is periodic with period $T = 2\pi/\omega$ and contains seven harmonics.

The signal actually used is a sampled signal defined at the sampling points

$$t = nh \quad h = T/320$$

The signal is obtained as follows:

$$u_1(t) = \begin{cases} a & u(t) > 0 \\ -a & u(t) < 0 \end{cases} \quad t = 0, h, \dots, 319h \quad (3.27)$$

Half a period of this signal is shown in Fig. 3.11.

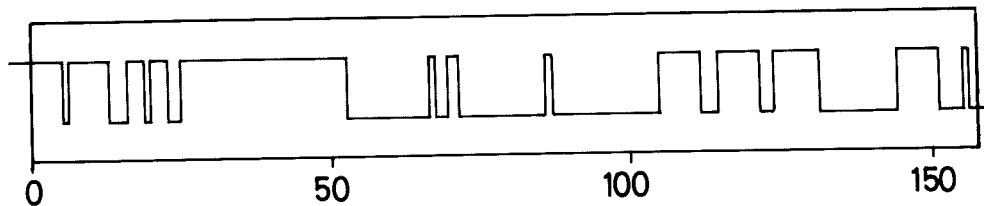


Fig. 3.11 - Half a period of Jensen's multifrequency signal. (Redrawn from Jensen (1959)).

Jensen has shown that the signal (3.26) has several nice properties. Most of the signal energy is contained at the 7 frequencies. It has also been demonstrated that the calculations required for correlating the input and the output can be organized efficiently.

Notice that Jensen's method is similar in spirit to the determination of the transfer function as the ratio of the Fourier transforms of the system output and the system input. Since efficient methods to compute Fourier transforms are now available (see Chapter 5), Jensen's method will not be elaborated further.

Exercises.

1. Consider a frequency response method where the amplitude and the phase are determined by fitting the parameters A and B of the function $v(t) = A \sin \omega t + B \cos \omega t$ to the output using least squares, which means that the function

$$\int_0^T [y(t) - A \sin \omega t - B \cos \omega t]^2 dt$$

is minimal. Show that this method is equivalent to the correlation method if $\omega T = n\pi$. (Compare with Ångström's method.)

2. Consider the correlation method for frequency analysis. Assume that the amplitude and phase are estimated from

$$\hat{y}_0 \cos \hat{\varphi} = 2y_s(t)/t$$

$$\hat{y}_0 \sin \hat{\varphi} = 2y_c(t)/t$$

Estimate the maximum error in the estimates obtained when t is arbitrary. How many periods are required in order to make the amplitude error less than 1% and the phase error less than 1° ? Disturbances in the output can be neglected.

3. Derive the formula (3.16) for the transfer function of the cosine channel.
4. Assume that the correlation method is used for frequency response analysis. Let the amplitude of the input signal be unity and assume that the error in the measurement of the output is white noise with spectral

density ϕ_0 . Determine the measurement error, give practically useful error estimates and show that the uncertainty in the transfer function can be represented as circles in a Nyquist diagram.

5. Consider Fig. 3.5. Explain why the outputs of the sine and cosine channels have a significant component of frequency 2ω in case A and of the frequency ω in case C. Compare also with Fig. 3.7.
6. Consider the results of Angström's experiment given in equations (3.24) and (3.25). Determine the thermal diffusivity by analysing the second and third harmonics. Compare with the results obtained for the first harmonics.
7. Simulate a frequency response analyser based on the correlation method and verify the results shown in Fig. 3.4 and Fig. 3.5.
8. Show that it is a coincidence that the estimates of the transfer function obtained for $t = \pi$ and $t = 3\pi$ in Fig. 3.4 are correct.
9. Show that if the sidebands are eliminated by using the window (3.17) then the transfer function associated with the sine channel is given by (3.13) with

$$G_1(s) = \frac{1}{sT(1-sT/2\pi)^2} (1-e^{-sT})$$

10. Simulate a frequency response analyser based on the correlation method and investigate the effects of a sinusoidal disturbance in the process output. In particular demonstrate the effect of the high sidebands and the use of a time window.

11. Find the effects on the frequency analyser of a disturbance in the process output of the form $n(t) = a + bt$.

4. TREND ELIMINATION.

It was shown in the previous section that the correlation method was very effective in eliminating the effects of disturbances in a frequency analysis. The analysis showed that the correlation channels could be interpreted as band pass filters whose center frequency was automatically equal to the frequency of the input signal. For integrating times equal to multiples of $2\pi/\omega_0$ it was also shown that the correlation channels could be characterized by the transfer functions (3.15) and (3.16). A series expansion of these transfer functions give

$$G_S(s) = \begin{cases} \frac{2}{\omega_0 T} - \frac{s}{\omega_0} + \dots & \omega_0 T = \pi, 3\pi, \dots \\ -\frac{s}{\omega_0} + \frac{s^2 T}{2\omega_0} + \dots & \omega_0 T = 2\pi, 4\pi, \dots \end{cases}$$

$$G_C(s) = \begin{cases} -\frac{2s}{\omega_0^2} + \frac{s^2}{\omega_0^2} + \dots & \omega_0 T = \pi, 3\pi, \dots \\ \frac{s^2}{\omega_0^2} - \frac{s^3 T}{2\omega_0^2} + \dots & \omega_0 T = 2\pi, 4\pi, \dots \end{cases}$$

The transfer function $G_C(s)$ will thus vanish for $s = 0$. The transfer function $G_S(0)$ is also equal to zero if $\omega_0 T = 2\pi, 4\pi, \dots$ i.e. if the integration is a multiple of the period of the input signal. Notice however that $G_S(0) = 2/(\omega_0 T)$ if $\omega_0 T = \pi, 3\pi, \dots$.

This means that a constant level in the output gives no error in the outputs of the correlation channels, if the integration time is chosen as a multiple of the period of the input signal.

A linear trend in the process output will, however, result in an error of the sine channel even if the integration time is chosen as a multiple of the period of the input signal. This is illustrated by the simulation results shown in Fig. 4.1. This figure shows the results obtained when analysing a system with the transfer function

$$G(s) = 1/(1+s)$$

The input signal is $u(t) = \sin t$, and a trend $n(t) = 0.1 t$ is added to the process output.

With no disturbance in the output it follows from (3.7) and (3.8) that the outputs of the correlation channels are

$$y_s(T) = T/4 \quad \omega_0 T = \pi, 2\pi, \dots$$

$$y_c(T) = T/4 \quad \omega_0 T = \pi, 2\pi, \dots$$

where n is a positive integer. Furthermore it follows from (4.1) that the drift $n(t) = 0.1 t$ will give the following contribution to the output of the sine channel

$$\hat{y}_s(T) = T G_s(p)n(T), \quad \omega_0 T = \pi, 2\pi, \dots$$

where p is the differential operator $p = d/dT$. Hence

$$\hat{y}_s(T) = \begin{cases} 0.1 T & \omega_0 T = \pi, 3\pi, \dots \\ -0.1 T & \omega_0 T = 2\pi, 4\pi, \dots \end{cases}$$

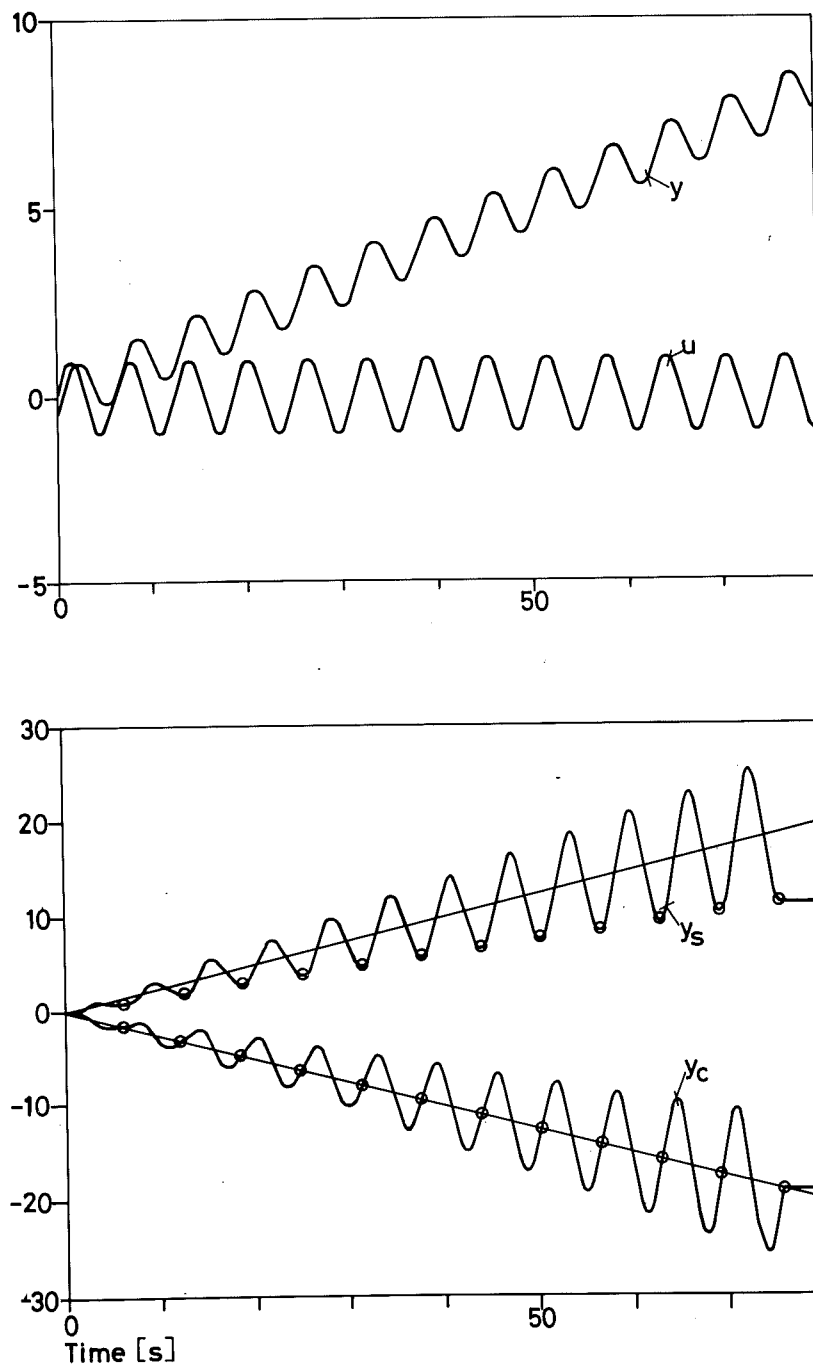


Fig. 4.1 - Results of simulation of frequency analysis based on correlation when there is a linear trend $0.1 t$ added to the process output. The input is $u(t) = \sin t$ and the system has the transfer function $G(s) = 1/(1+s)$. Notice that there is a bias in the sine channel and no error in the cosine channel as can be expected from (4.1) if the integration time is a multiple of the period of the input signal.

The output of the sine channel in the presence of the drift thus becomes

$$y_s(T) = \begin{cases} 0.35 T & \omega_0 T = \pi, 3\pi, \dots \\ 0.15 T & \omega_0 T = 2\pi, 4\pi, \dots \end{cases}$$

Compare with the results of the simulation shown in Fig. 4.1. The simple calculation illustrates the usefulness of the transfer functions G_s and G_c to get insight and error estimates.

Persson's Device.

A technique to eliminate the effects of drift and other low frequency disturbances will now be discussed. Assume for example that the measurement error is a polynomial in t of degree ℓ . In principle such a disturbance could be eliminated by performing the frequency analysis of the signal, obtained by differentiating the output signal $\ell+1$ times. Such a solution will, however, increase the high frequency noise considerably. A similar scheme, which does not introduce high frequency disturbances, would be to calculate the integrals y_s (3.5) and y_c (3.6) over separate half periods and to take differences of order $\ell+1$. Schemes of this type have been used when analysing nuclear reactors. See Schmid (1956). The particular method described here is due to Rolf Persson (1955).

Consider the output of the sine channel of the system and assume that the integration time is chosen in such a way that ωT is an integer multiple of π , say $\omega T = N\pi$. The output of the sine channel then becomes

$$\begin{aligned} y_s &= \int_0^T y(t) \sin \omega t \, dt = \frac{1}{\omega} \int_0^{\omega T} y\left(\frac{\tau}{\omega}\right) \sin \tau \, d\tau = \\ &= \frac{1}{\omega} \sum_{k=1}^N \int_{(k-1)\pi}^{k\pi} y\left(\frac{\tau}{\omega}\right) \sin \tau \, d\tau \end{aligned} \quad (4.3)$$

The basic idea used to eliminate the effects of trends is to modify the frequency response analyser so that the output is given by

$$\tilde{y}_s = \frac{1}{\omega} \sum_{k=1}^N \alpha_k \int_{(k-1)\pi}^{k\pi} y\left(\frac{\tau}{\omega}\right) \sin \tau d\tau \quad (4.4)$$

instead of (4.3). It will be shown that the parameters α_k can be chosen in such a way that an error in the output in the form of a polynomial will not have any effect on the function \tilde{y}_s .

Assume that there is an error in the process output which is a polynomial in t of degree ℓ . Since

$$\begin{aligned} I_\ell &= \int_{(k-1)\pi}^{k\pi} \tau^\ell \sin \tau d\tau = (-1)^{k-1} \pi^\ell [k^\ell + (k-1)^\ell] - \\ &\quad - \ell(\ell-1) I_{\ell-2} \end{aligned}$$

we find that the polynomial error will give the contribution

$$\tilde{e}_s = \sum_{k=1}^N \alpha_k (-1)^{k-1} P_\ell(k) \quad (4.5)$$

to the output of the sine channel, where $P_\ell(k)$ is a polynomial of degree ℓ in k . Notice that the coefficients of the polynomial do not depend on k ! Now let q denote a shift operator in k defined by

$$qP(k) = P(k+1) \quad (4.6)$$

For any polynomial of degree less than or equal to ℓ we have the identity

$$(q-1)^{\ell+1} P_{\ell}(k) = 0 \quad (4.7)$$

Hence if the coefficients α_k in (4.4) are selected in such a way that the linear operation defined by (4.4) corresponds to the difference scheme (4.7) we get

$$\tilde{e}_s = \sum_{k=1}^N \alpha_k (-1)^{k-1} P_{\ell}(k) = \left[(q-1)^{\ell+1} P_{\ell}(k) \right]_{k=1} = 0 \quad (4.8)$$

This is possible if $N = \ell+2$ and if the coefficients are chosen proportional to the binomial coefficient

$$\alpha_k = \binom{\ell+1}{k-1} = \frac{(\ell+1)!}{(k-1)! (\ell-k+2)!} \cdot 2^{-(\ell+1)} \quad (4.9)$$

The coefficients are normalized in such a way that their sums equal one.

In the particular case of a linear trend we have $\ell = 1$, $N = 3$ and $\alpha_1 = 1$, $\alpha_2 = 2$ and $\alpha_3 = 1$.

Fig. 4.2 shows a simulation of the trend elimination scheme (4.4) with the parameters given above.

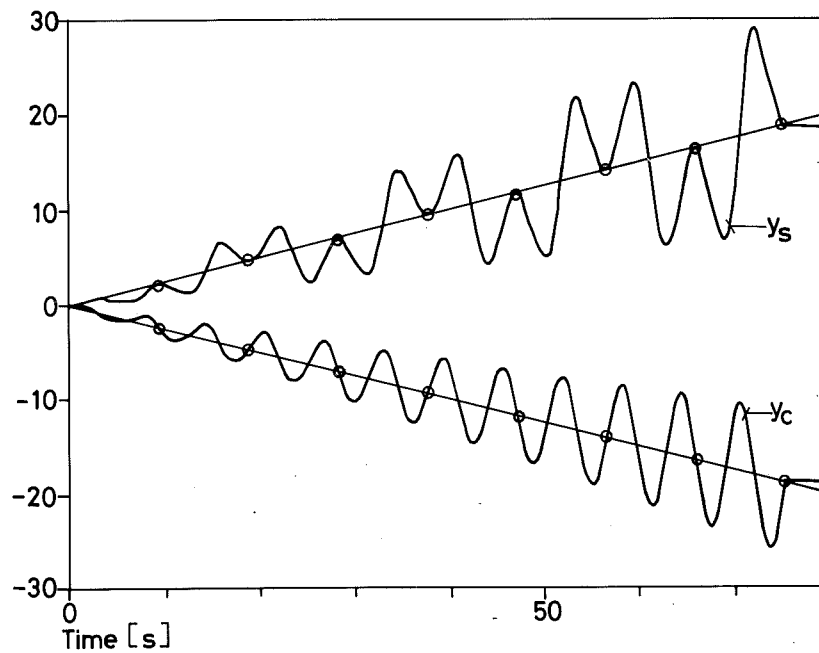


Fig. 4.2 - Outputs of the sine and cosine channels for a frequency analyser with trend elimination in the sine channel. The system has the transfer function $G(s) = 1/(1+s)$, the input is $u(t) = \sin t$ and the trend $0.1 t$ is added to the output.

Exercises.

1. Consider the correlation method. Assume that the output is disturbed by a constant level. Determine the errors in the sine and cosine channels for $\omega_0 T = \pi, 3\pi, \dots$ and $\omega_0 T = 2\pi, 4\pi, \dots$.
2. Simulate a frequency analyser when there is a trend error in the system output and verify the results shown in Fig. 4.1 and Fig. 4.2.

5. SAMPLED SYSTEMS.

Many systems of practical interest have parts which correspond to sampled systems. Typical examples are control systems with computers or special digital devices. Other examples are systems where signals are transmitted digitally. Such systems are found both in technical and biological applications. Certain processes like internal combustion engines have mechanisms like the ignition system which are naturally described as sampled systems due to their physical nature.

There is a fundamental difficulty in trying to identify a sampled data system because such systems are not time invariant. If the sampling is periodic the systems are periodic with a period equal to the sampling interval. The notion of transfer function which is properly defined only for time invariant system thus must be used with some care. The periodicity is usually avoided in the analysis by considering the values of the system variables only at discrete times which are synchronized to the sampling instants.

The fact that sampled systems are not time invariant implies that the steady state output generated by a sinusoidal input will have components with frequencies different from the frequency of the input signal. The effects are particularly pronounced at frequencies approaching half the sampling frequency.

There are several cases reported in the literature where difficulties have been encountered by ignoring the time varying nature of sampled systems.

Frequency Analysis.

The difficulties associated with frequency analysis of a sampled data system will now be demonstrated in a simple case. Consider the system shown in Fig. 5.1 consisting of a sampler and a linear time invariant system with the transfer function $G(s)$.

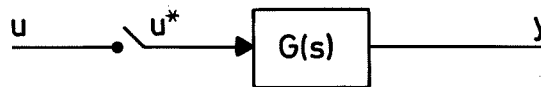


Fig. 5.1 - Block diagram of a simple system with a sampler.

It is assumed that the reader is familiar with the basic concepts of classical sampled data theory. See Ragazzini and Franklin (1958).

An idealized model of the sampler gives the sampled output as

$$u^*(t) = u(t)S(t) \quad (5.1)$$

where $S(t)$ is a train of impulses which is formally written as

$$S(t) = \sum_{n=-\infty}^{\infty} \delta(t-nT) = \frac{1}{T} \left[1 + 2 \sum_{n=1}^{\infty} \cos n\omega_s t \right] \quad (5.2)$$

where T is the sampling period and $\omega_s T = 2\pi$.

Let the input signal to the sampler be

$$u(t) = \sin(\omega t + \varphi)$$

The output then becomes

$$\begin{aligned} u^*(t) &= \frac{1}{T} \left[\sin(\omega t + \varphi) + 2 \sum_{n=1}^{\infty} \cos(n\omega_s t) \sin(\omega t + \varphi) \right] = \\ &= \frac{1}{T} \left\{ \sin(\omega t + \varphi) + \sum_{n=1}^{\infty} [\sin(n\omega_s t + \omega t + \varphi) - \right. \\ &\quad \left. - \sin(n\omega_s t - \omega t - \varphi)] \right\} \end{aligned}$$

Notice that the sampled signal u^* can be considered as the modulation of u with the impulse train S . The sampled signal u^* contains components with the frequency ω and with the side-band frequencies $n\omega_s \pm \omega$. See Fig. 5.2.

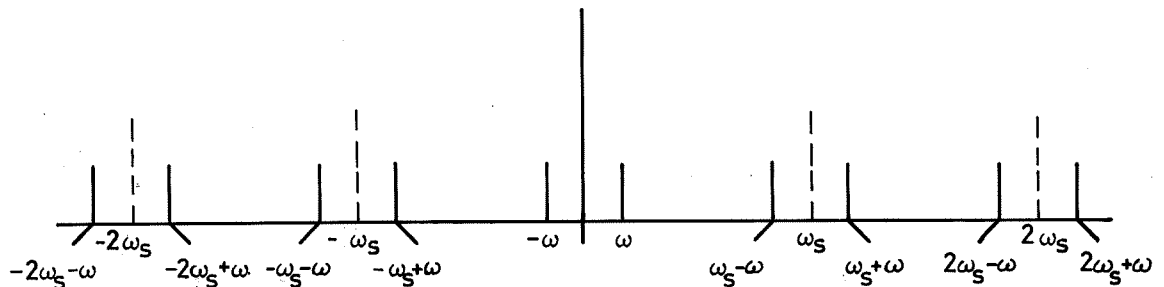


Fig. 5.2 - Illustrates the frequency content of the signal obtained by sampling a sine-wave with frequency ω .

The output signal is easily obtained by superposition.
Hence

$$y(t) = \frac{1}{T} \operatorname{Im} \left\{ G(i\omega) e^{i(\omega t + \varphi)} + \sum_{n=1}^{\infty} G(i(n\omega_s + \omega)) e^{i(n\omega_s t + \omega t + \varphi)} - \right. \\ \left. - G(i(n\omega_s - \omega)) e^{i(n\omega_s t - \omega t - \varphi)} \right\} \quad (5.3)$$

The output thus has components of the fundamental frequency ω as well as side-bands $n\omega_s \pm \omega$. These components will in general be filtered out when performing a frequency analysis. For $\omega = n\omega_s/2$ the frequency of one of the side-bands will, however, coincide with the frequency of the input signal. The component of the output with the same frequency as the input (the fundamental component) is then given by

$$\begin{aligned} \tilde{y}(t) &= \frac{1}{T} \operatorname{Im} \left\{ G(i\omega) e^{i(\omega t + \varphi)} - G(i\omega) e^{i(\omega t - \varphi)} \right\} = \\ &= \frac{1}{T} \operatorname{Im} \left\{ (1 - e^{-2i\varphi}) G(i\omega) e^{i(\omega t + \varphi)} \right\} = \\ &= \frac{1}{T} \operatorname{Im} \left\{ 2e^{i(\pi/2 - \varphi)} \sin \varphi G(i\omega) e^{i(\omega t + \varphi)} \right\}, \quad \omega = n\omega_s/2 \quad (5.4) \end{aligned}$$

For $\omega \neq n\omega_s/2$ the fundamental component of the output (5.3) is

$$\tilde{y}(t) = \frac{1}{T} \operatorname{Im} \left\{ G(i\omega) e^{i(\omega t + \varphi)} \right\} \quad (5.5)$$

Hence if a frequency analysis is performed by exciting the system with a sine-wave and if the amplitude and phase relations between the fundamental component of the input and the output are measured the following estimate of the transfer function is obtained

$$\hat{G}(i\omega) = \begin{cases} \frac{1}{T} G(i\omega) & \omega \neq n\omega_s/2 \\ \frac{2}{T} e^{i(\pi/2 - \varphi)} \sin \varphi G(i\omega) & \omega = n\omega_s/2 \end{cases} \quad (5.6)$$

A frequency response analysis of the sampled data system shown in Fig. 5.1 will thus give the estimate $\hat{G} = G/T$ for all frequencies except those which are multiples of the Nyquist frequency ($\omega_s/2$). At frequencies $n\omega_s/2$ the estimate of the transfer function will depend on the way the sinusoidal input is synchronized to the sampling instants. For $\phi = 0$ the estimate is $\hat{G} = 0$ while $\phi = \pi/2$ gives $\hat{G} = 2 G/T$ and $\phi = 3\pi/2$ gives $\hat{G} = -2 G/T$. If it is attempted to measure the value of the transfer function at $\omega = n\omega_s/2$ and if great care is not taken to synchronize the sine-wave with the sampling frequency the points will be widely scattered.

Finite Measurement Time.

In the analysis performed it was assumed that the equipment used for the frequency analysis was perfect in the sense that the fundamental component is perfectly separated from the side-bands. In practice it may happen that the side-bands are picked up. The estimated \hat{G} will then be different from G/T also at frequencies different from $n\omega_s/s$. For example, if a frequency analyser based on correlation is used to analyse the system shown in Fig. 5.1, it can be shown that the lower side-bands ($n\omega_s - \omega$) will give a significant contribution even if the integration time is fairly long. It follows from equation (5.3) that the contribution due to the frequency $n\omega_s - \omega$ will depend on ϕ i.e. the synchronization of the sine wave with respect to the sampling periods. A noticeable scatter of the estimates will thus be observed if the sine wave is not synchronized to the sampling intervals. Empirically it has been found that the effect is noticeable at frequencies above $\omega_s/4$. See Fig. 5.3.

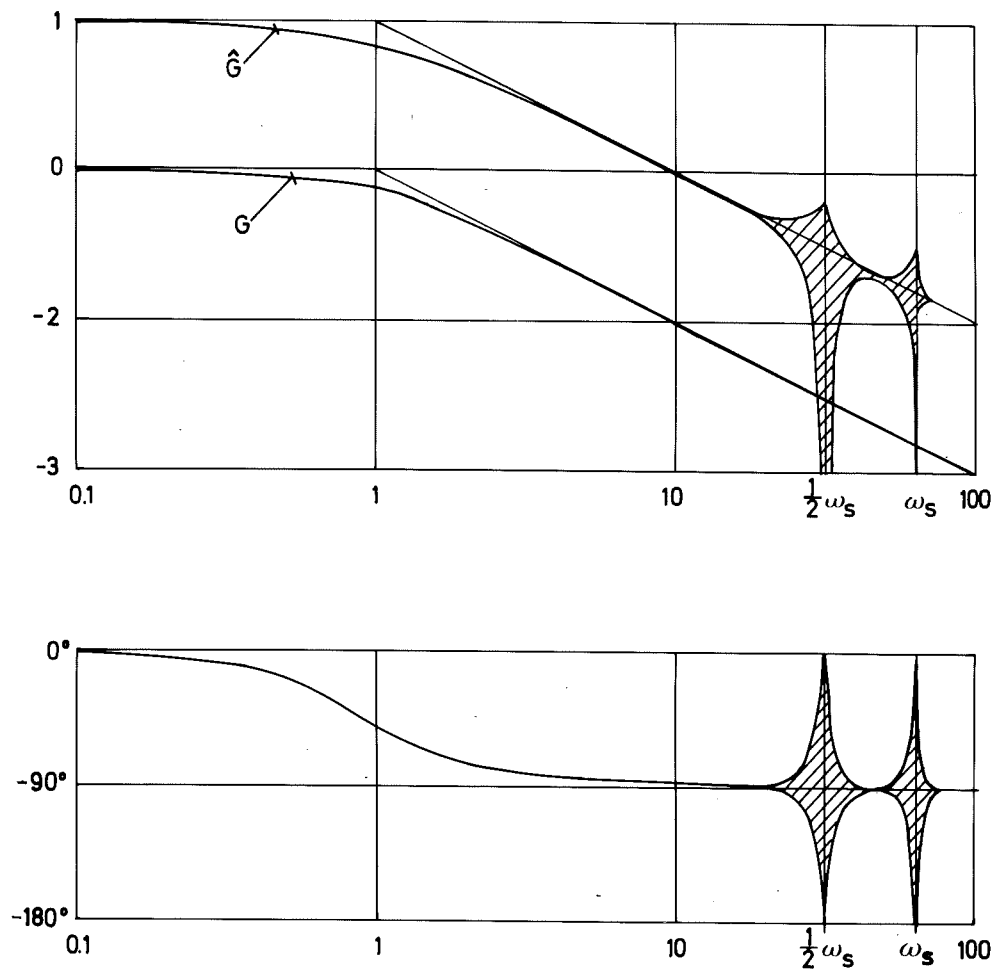


Fig. 5.3 - Results of frequency response analysis using the correlation method applied to a system consisting of a sample and hold followed by a system with the transfer function $1/(1+s)$. The sampling frequency is 10 Hz (≈ 62.8 rad/s). Depending on the synchronization between the input and the sampling, any values in the shaded region can be obtained. The integration time is 5 cycles.

Diesel Engine Dynamics.

A diesel engine is intrinsically a sampled data system because of the ignition mechanism. To explain this let T denote the time for the motor to complete one cycle. The fuel injection time is so short in comparison with T that it can be considered as instantaneous. The ignition comes after a certain delay and results in a torque-pulse which lasts for about $T/4$. The area of the torque-pulse is proportional to the injected fuel. The torque-pulse results in a motion of the motor which is determined also by the moment of inertia of the load and the damping. For the purpose of control the diesel engine can be considered as a system whose input is the setting of the fuel rack which determines the injected fuel and whose output is angular velocity. In early models the sampled nature of the system was disregarded, and the motor was simply described by the transfer function

$$G(s) = \frac{K}{Js + D} e^{-sT_d} \quad (5.7)$$

where K is the mean torque per fuel flow rate, J the moment of inertia, D the damping and T_d the time between firing strokes. A significantly different model is obtained when the diesel engine is modelled as a sampled system. The model will, for example, critically depend on the number of cylinders.

For a long time diesel engines were studied using frequency response methods. The transfer functions obtained were reproducible for low frequencies, up to about a quarter of the sampling frequency. The sampling frequency is the ratio of the number of independently fired cylinders and the time required for a full cycle. At higher frequencies, however, a large scatter in the estimates of the

transfer function was observed. This problem was not resolved until the consequences of the sampled nature of the diesel engine were analysed by Bowns (1971). Frequency analysis was also applied by Flower (1973) who applied correlation techniques. By using a synchronization device which starts the correlation at a coincidence of a positive zero crossing of the sine wave with an ignition, it was possible to obtain reproducible results for frequencies higher than the sampling frequency. This gives a specified value to ϕ in (5.6).

The experiment was performed on a closed loop system consisting of a motor with governor. The input was chosen as the reference value of the speed governor, see Fig. 5.4. A sample of the results obtained is shown in the Bode diagram of Fig. 5.5. The results cannot be well explained by the continuous time model (5.7).

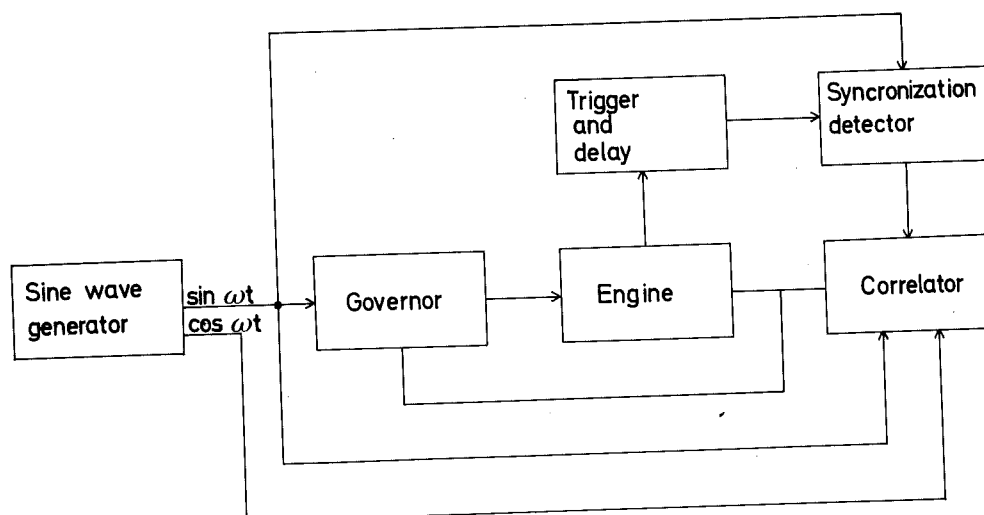


Fig. 5.4 - Arrangement used by Flower to determine the transfer function of a diesel engine. The correlation method was used and the integration was started when the input signal zero crossing coincided with the ignition impulse suitably delayed. (Redrawn from Windett and Flower (1973)).

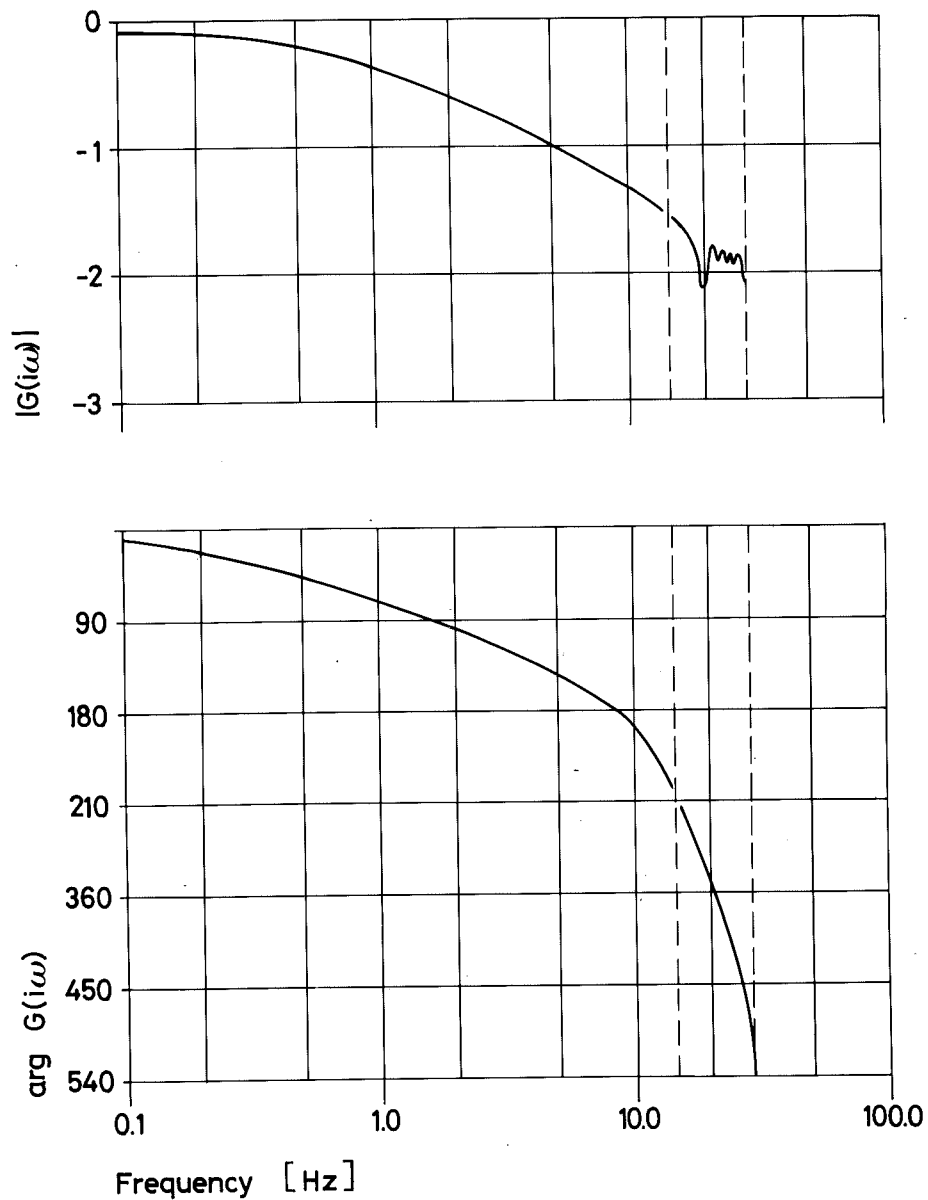
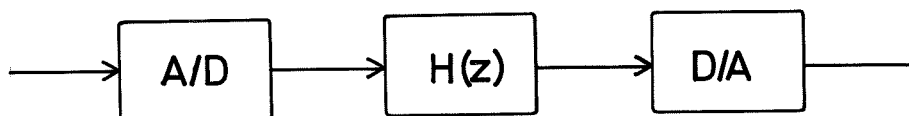


Fig. 5.5 - Frequency response of a diesel engine running at 600 RPM.

The motor is a six-cylinder, four-stroke engine which means that $f_s = 30$ Hz. The correlation method is used and the input synchronized for measurements above 7.5 Hz. The integration time used was 100 cycles. (Redrawn from Windett and Flower (1973)).

Exercises.

1. Consider the sampled data system shown in the figure below which consists of an analog to digital converter, an algorithm characterized by the pulse transfer function $H(z)$ implemented on a digital computer, and a digital to analog converter which holds the previous value until a new value is received.



Assume that the input signal is a sinusoid

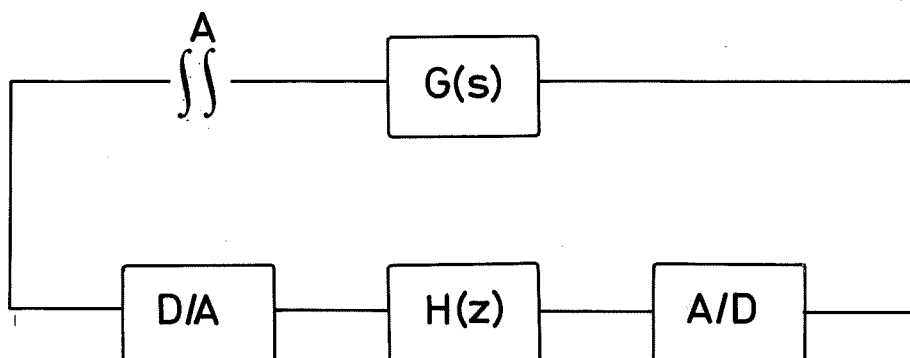
$$u(t) = \text{Im}\{e^{i(\omega t + \phi)}\}$$

Show that the output of the analog to digital converter in the steady state can be written as

$$y(t) = \text{Im}\left\{\sum_{n=-\infty}^{\infty} \frac{1}{(i\omega + in\omega_s)T} (1 - e^{i\omega T}) H(e^{i\omega T}) e^{i(\omega t + n\omega_s t + \phi)}\right\}$$

Discuss what would happen if it was attempted to analyse the system with a frequency response analyser.

2. Consider the digital control system illustrated by the block diagram below



Assume that the loop is broken at the point A and that a frequency response analysis is performed by sending in a sinusoid and measuring the amplitude and phase relation between the input and the fundamental component of the output. How can the result be used to analyse the stability of the closed loop system?

3. Assume that the system in Fig. 5.1 is analysed by frequency response based on correlation. Neglect all frequencies in the output given by (5.3) except the fundamental ω and the first side-band $\omega_s/2 - \omega$. Determine the output of the sine and cosine channels and analyse how the result depends on the synchronization of the input to the sampling intervals.
4. Simulate frequency response of a sampled system and verify qualitatively the results shown in Fig. 5.3. Also analyse the signal wave forms.

6. SUMMARY.

Frequency response is a very flexible and useful tool for determination of the transfer function of a linear system. The method is also useful in order to explore the region in which a system can be considered as linear. Frequency response is also conveniently used to find the model complexity required to describe the dynamics of a system over a given range of frequencies.

Frequency response requires very little equipment. For high signal to noise ratios a sine-wave generator and a two channel recorder is sufficient. By using correlation techniques with time windows and trend elimination the method can also be used for very low signal to noise ratios.

The transfer function is obtained directly during the experiment without extensive calculations. This is very convenient because measurement can be repeated if doubts occur and the experiment can be planned adaptively exploiting previous results.

The only case when it is very inconvenient to use frequency response is when analysing systems with very long time constants. In such a case it takes a long time to wait for steady state and to make measurements for many frequencies, particularly if the signal to noise ratio is so low that the correlation method must be used.

7. ACKNOWLEDGEMENTS.

I am grateful to Mr. E. Persson of the ASEA company for letting me share some of his knowledge, insights and experiences of frequency response analysis. I also wish to thank my co-workers Ivar Gustavsson, Per Hagander, Sture Lindahl, Gustaf Olsson, Jan Sternby and Björn Wittenmark who have critically read different versions of the manuscript. Many thanks are due to Mrs. Gudrun Christensen and Mrs. Marianne Moore who typed the manuscript and to Miss Britt-Marie Carlsson who prepared the figures.

8. NOTES AND REFERENCES.

Frequency response analysis is extensively used and well covered in literature. It was applied by the physicist Angström as early as 1861. After the discovery of the Nyquist theorem, frequency analysis was a standard tool in the design of electronic amplifiers. A typical example is given in Bode (1945, p. 491-492). In the field of automatic control frequency analysis was used before World War II by Charles Stark Draper in his investigations of dynamics of aircraft instrumentation reported in Draper (1953) and by Gordon Brown in studies of hydraulic transmissions. A good source for the early work is Oldenburger (1955) which contains original papers and many references. Frequency analysis is now a very useful standard tool which has been applied to a large variety of technical and nontechnical systems.

The submarine example discussed in Section 2 is taken from Garde and Persson (1960) and from material which has been kindly supplied by the Royal Swedish Navy. Determination of aircraft dynamics by frequency response is described in Campbell (1947).

Frequency response has also been widely used in investigations of chemical processes; a survey is given in Williams (1961), which contains many references. A typical application is given by Hoiberg et al (1971). They investigate the dynamics of a fixed-bed reactor producing water from hydrogen and oxygen.

Frequency response has been applied to several physiological systems. Several examples are given in Milhorn (1966). The example on pupillatory light reflex dynamics is based on Stark (1958, 1968). In Herman and Stark (1963) frequency response analysis is used to investigate the dynamics of

a single photoreceptor neuron. When investigating the pupillary light reflex dynamics it was possible to open the loop in a very elegant manner. In general it is, however, very difficult to open the loop in a physiological system. Most frequently it is necessary to use surgery. A typical example is given in a sequence of papers by Sawaga et al (1961, 1962). The control loop which regulates cerebral blood flow by changing systemic arterial pressure was investigated. Two dogs were used in the experiment. The blood vessels supplying the blood to the brain of dog A were cut and connected to dog B in such a way that the blood flow through the brain of dog A could be regulated. Frequency response was applied by varying the blood flow to the brain of dog A and by measuring the response in systemic arterial pressure of the same dog. In this way the open loop transfer function was obtained. The gain necessary to give an unstable closed loop system was calculated from the open loop measurements. The results were verified by connecting the signal from the blood pressure measurement to the flow regulator through an amplifier. Frequency response has also been used in investigations of the circulatory system by Grodins (1963).

Frequency response analysis of nonlinear systems is discussed in Graham and McRuer (1961). The measurements on the Swedish power network discussed in Section 3 were done by Almström and Garde (1950). The work is also described in Oja (1955). Application of frequency response to control of water turbines are discussed in Hutarew (1969).

The section on determination of thermal conductivity of metals is based on Ångström (1861). Ångström's method, which has been rediscovered several times, is a standard method to determine thermal diffusivity. Extensive discussions are found in the classic Carslaw and Jaeger (1959)

and the more practically oriented monograph Tye (1969). A recent application of more advanced parameter estimation methods to the determination of thermal conductivity is given in Leden (1973).

The trend elimination device discussed in Section 4 is due to Rolf Persson (1955). It was developed in connection with frequency analysis of nuclear reactors. A review of trend elimination schemes is given in Schmid (1956). Frequency analysis has in fact become one of the standard methods for analysing the dynamics of a nuclear reactor. The reactivity of the reactor is varied sinusoidally, and the corresponding change in neutron flux is measured. Early determinations of zero power transfer functions were carried out in Chalk River and Argonne National Laboratory before 1950. For measurements on low power graphite moderated reactors the simple amplitude and phase comparison discussed in Section 1, can be used because the neutron flux signal is virtually noise free. For boiling water reactors the situation is very different, because the boiling generates noise in the flux signal (5% of the total signal). In such a case the correlation method is used. See Schmid (1956). To generate the sinusoidal variations in reactivity, a special control rod, often called pile oscillator, is used. In a typical case such a reactivity oscillator is composed of a rotor and a stator, on which are mounted sine and rectangular shaped strips of an absorber. When the sine strip is rotated with respect to the rectangular strip at a constant speed, a sinusoidal variation in reactivity is obtained. The frequency is changed by changing the speed of rotation. Typical frequencies that are used in the experiment are 0.002 - 10 Hz. A general survey is found in Harrer (1963). More details are given in DeShong (1960) and in Tosi and Åkerhielm (1964).

The multifrequency method described in Section 3 is described in Jensen (1959). Jensen's notes contain much interesting material on frequency analysis. The test signals proposed by Jensen have the interesting property that their power is concentrated at narrow bands around a fixed number of frequencies. Further aspects on the generation of such signals are found in van den Bos (1967, 1970).

Application of frequency response analysis to modelling of diesel engines is described in Welbourn et al (1959). A sample data model for the diesel engine is given in Bowns (1970). This paper also contains results of experimental frequency analysis. Frequency response of sampled systems is also discussed in Flower et al (1971). An application to diesel engines is given in Windett and Flower (1973).

Frequency response analysers have been implemented in many different ways. Using the technology available before 1960, the generation of low frequency sinusoids was difficult. Much ingenuity therefore went into the design of such equipment, see St. Clair et al (1955), Ahrendt (1960), Balchen (1962), Hutarew (1969). With the technology that is available today the implementation of low frequency sine wave generators and correlators is straightforward. Equipment for frequency response analysis is now available from many instrument suppliers. A review of available equipment is given in Strobel (1967).

A frequency response analyser can, of course, also be easily implemented on a minicomputer with A/D and D/A converters or with an interface to a sine cosine signal generator. See Persson (1973). Using such an implementation it is easy to incorporate effective filtering procedures to eliminate both drift and high frequency disturbances.

Ahrendt, W. R., Savant, C. J. (1960)

"Servomechanism Practice", McGraw-Hill, New York

Almström, K., Garde, A. (1950)

"Electrohydraulic Regulation of Water-Turbines, Part 3, Investigation by Frequency Analysis of the Swedish Network", Proc. CIGRE, Session 1950, 29 June - 8 July, 315, 23-36.

Balchen, J. G. (1962)

"Ein Einfaches Gerät zur experimentellen Bestimmung des Frequenzganges von Regelungstechnik", Regelungstechnik 10, p. 200-205.

Bode, H. W. (1945)

"Network Analysis and Feedback Amplifier Design", Van Nostrand, Princeton, N.J.

van den Bos, A. (1967)

"Construction of Binary Multifrequency Test Signals", Paper 4.6. Preprints IFAC Symposium on Identification in Automatic Control Systems, Prague, June 1967, Academia Prague.

van den Bos, A. (1970)

"Estimation of Linear System Coefficients from Noisy Responses to Binary Multifrequency Test Signals", Paper 7.2. Preprints 2nd IFAC Symposium on Identification and Process Parameter Estimation, Prague, June 1970, Academia Prague.

Bowns, D. (1971)

"The Dynamic Transfer Characteristics of Reciprocating Engines", Proc. Inst. Mech. Engrs. 185, 185-201.

Campbell, G. F., Whitcomb, D. W., Brenhaus, W. O. (1947)
 "Dynamic Longitudinal Stability and Control Flight Tests of a B-25J Airplane- Forced Oscillation and Step Function Response Methods, Utilizing an A-12 Automatic Pilot", Report TB-405-F-3, Cornell Aero. Lab., April, (USAF Techn. Rep. 5688).

Carslaw, H. S., Jaeger, J. C. (1959)
 "Conduction of Heat in Solids", Clarendon Press, Oxford.

De Shong, J. A., Jr. editor (1960)
 "Proc. Conf. on Transfer Function Measurements and Reactor Stability Analysis", Argonne National Lab. Argonn III, Report ANL-6205, AEC Rand C. Available from OTS, Dept. of Commerce, Washington, D.C.

Draper, C. S., McKay, W., Lees, S. (1953)
 "Instrument Engineering", Vol. 1, 2, and 3, McGraw Hill, New York.

Elmqvist, H. (1975)
 "SIMNON- Users Guide", Report 7502, Department of Automatic Control, Lund Institute of Technology.

Flower, J. O., Windett, G. P., Forge, S. C. (1971)
 "Aspects of the Frequency Response Testing of Simple Sampled Systems", Int.J. Control 14, 881-896.

Garde, A., Persson, E. (1960)
 "Automatisk djupstyrning av ubåtar", (Automatic Depth Control of Submarines), ASEA tidning 52, 127-131.

Goldsmith, A., Waterman, T. E., Hirschhorn, H. J. (1961):
 "Handbook of Thermodynamical Properties of Solid Materials",
 Pergamon Press, Oxford.

Graham, D., McRuer, D. (1961)
 "Analysis of Nonlinear Control Systems", Wiley, New York.

Grodins, F. S. (1963)
 "Control Theory and Biological Systems", Columbia Univ.
 Press, New York.

Harrer, J. M. (1963)
 "Nuclear Reactor Control Engineering", Van Nostrand,
 Princeton, N. J.

Hermann, H. T., Stark, L. (1963)
 "Photoreceptor Unit Transfer Characteristics", J. Neuro-
 physiology 26, 215-228.

Hoiberg, J. A., Lyche, B. C., Foss, A. S. (1971)
 "Experimental Evaluation of Dynamic Models for a Fixed-
 Bed Catalytic Reactor", AIChE Journal 17, 1434-1447.

Hutarew, G. (1969)
 "Regelungstechnik - Kurze Einführung am Beispiel der
 Drehzahlregelung von Wasserturbinen", Springer-Verlag,
 Berlin.

Jensen, J. R. (1959)
 "Notes on the Measurement of Dynamic Characteristics of
 Linear Systems - Part III", Copenhagen.

Leden, B., Hamza, M. H. Sheirah, M. A. (1973)

"Different Methods for Estimation of Thermal Diffusivity of a Heat Diffusion Process", Paper TD-1, Proc. 3rd IFAC Symposium on Identification and System Parameter Estimation, North Holland Amsterdam, 639-648.

Milhorn, H. T. (1966)

"The Application of Control Theory to Physiological Systems", W. B. Saunders Company, Philadelphia, Pennsylvania.

Oja, V. (1955)

"Frequency - Response Method, Applied to the Study of Turbine Regulation in the Swedish Power System", In Oldenburger (1955), 109-117.

Oldenburger, R. (editor) (1955)

"Frequency Response", MacMillan, New York.

Persson, C. (1973)

"Frekvensanalys". LTH (MA Thesis), Report RE-122, Department of Automatic Control, Lund Institute of Technology, June 1973.

Persson, E. (1967)

"Private Communication".

Persson, R. (1955)

See Schmid (1956)

Ragazzini, J. R. and Franklin, G. F. (1958)

"Sampled Data Control Systems", McGraw Hill, New York.

Sawaga, K., Taylor, A. E., Guyton, A. C. (1961)

"Dynamic Performance and Stability of Cerebral Ischemic Pressor Response", Am. J. Physiol. 201, 1164-1172.

Sagawa, K., Carrier. O., Guyton, A. C. (1962)

"Elicitation of the Theoretically predicted Feedback Oscillation in Arterial Pressure", Am. J. Physiol. 203, 141-146.

Schmid, P. (1956)

"High Precision Detector for Periodic Power Modulation in JEEP", Report 42, Joint Establishment for Nuclear Energy Research, Kjeller, Norway, Jan. 1956.

Stark, L. (1959)

"Stability, Oscillations and Noise in the Human Pupil Servomechanism", Proc. IRE 47, 1925-1939.

Stark, L. (1968)

"Neurological Control Systems - Studies in Bioengineering", Plenum Press, New York.

St. Clair, D. W., Erath, L. W., Gillespie, S. L. (1955)

"Sine-Wave Generators - A Survey of Pneumatic, Mechanical and Electrical Devices for Obtaining Frequency - Response Data" In Oldenburger (1955), 70-77.

Strobel, H. (1967)

"Systemanalyse mit determinierten Testsignalen", VEB Verlag Technik, Berlin.

Tosi, V., Åkerhielm, F. (1964)

"Sinusoidal Reactivity Perturbation Experiments with the HWBR

Second Fuel Charge", Report HPR 49. OECD Halden Reactor Project, Halden Norway.

Tye, R. P. (1969)

"Thermal Conductivity", Academic Press, New York.

Welbourn, D. B., Roberts, D. K., Fuller, R. A. (1959)

"Governing of Compression - Ignition Oil Engines", Proc. Inst. Mech. Engrs. 173, 575-604.

Williams, T. J. (editor) (1961)

"Process Dynamics and Control", Chemical Engineering Progress Symposium Series, Vol. 57.

Windett, G. P., Flower. J. O. (1973)

"Sampled-data Frequency Response Measurements of a Large Diesel Engine", Report, Univ. of Sussex, Brighton, March 1973.

Ångström, A. I. (1861)

"Neue Methode, das Wärmeleitungsvermögen der Körper zu bestimmen", Annalen der Physik und Chemie 114, 513-530.

APPENDIX A - SIMULATION PROGRAMS.

This appendix gives computer programs for a frequency analyser and programs which have been used to simulate the analyser in different situations. The programs were used to generate several of the figures in this chapter. They are also useful for the solution of some of the exercises. The programs are written in the interactive simulation language SIMNON described in Elmqvist (1975). There should, however, be little difficulty to rewrite the programs in any other language.

A1. Jump Resonance.

To simulate the jump resonance phenomenon shown in Fig. 2.17 a system SSERV representing the saturating servo shown in Fig. 2.16 was generated. The sinusoidal input was generated in the connecting system INSI. The program listings for these programs are given below.

CONTINUOUS SYSTEM SSERV "SERVO WITH SATURATION

INPUT U
OUTPUT Y
STATE X1 X2
DER DX1 DX2

INITIAL
X1:0
X2:0
A1=-A

OUTPUT
Y=X1

DYNAMICS
E=U-Y
M1=MIN(E,A)
M=MAX(M1,A1)
DX1=X2
DX2=-0.2*(X2-K*M)

A:1
K:20

END

CONNECTING SYSTEM INSI "SINE GENERATOR

TIME T

U[SSERV]=A*SIN(W*T)

A:0.5
W:1.3

END

To carry out the simulation and to generate Fig. 2.17 the following dialogue was performed using SIMNON.

```
>SYST SSERV INSI  
>AXES H 0 50 V -4 8  
>PLOT Y  
>SIMU 0 50  
>INIT X1:8  
>SIMU  
>
```

A2. A Frequency Analyser.

The program for a system representing a frequency analyser using the correlation method FREQA is listed below. The program listing is largely self explanatory. The system FREQA generates a sinusoidal input, performs the correlation and computes the magnitude and phase angle of the transfer function. There are options to eliminate sidebands by using the time window (3.17) and for trend elimination as was described in Section 4.

CONTINUOUS SYSTEM FREQA

"FREQUENCY ANALYSER

"FREQUENCY ANALYSER USING THE CORRELATION METHOD

"THE ANALYSER GENERATES THE INPUT $U=A*\sin(W*T)$ TO BE APPLIED
 "TO THE SYSTEM AND CALCULATES THE TRANSFER FUNCTION USING THE
 "CORRELATION METHOD

"THERE ARE THREE SETTINGS

" 1 SIGNAL AMPLITUDE A

" 2 FREQUENCY W

" 3 INTEGRATION TIME (SPECIFIED AS NUMBER OF PERIODS NP)

"THERE ARE THREE OPTIONS

" 1 TIME WINDOW $1-\cos(2*\pi*T/TI)$ TO ELIMINATE SIDEBANDS

" ACTIVATED BY SETTING THE PARAMETER CW:1.

" 2 TREND ELIMINATION IN SINE CHANNEL USING PERSSONS DEVICE

" ACTIVATED BY SETTING YP>0

INPUT Y

OUTPUT U ARGG ABSG

TIME T

STATE YS YC

DER DYS DYC

INITIAL

YS:0

YC:0

$TI=NP*2*\pi/W$

$TEPS=TI*1E-4$

$TP=\pi/W$

OUTPUT

$S=A*\sin(W*T)$

$C=A*\cos(W*T)$

U=S

$T1=\min(T, TI)$

$T2=\max(T1, TEPS)$

$ABSG=\sqrt{4*(YS*YS+YC*YC)}/T2$

$ARGG=ATAN2(YC, YS)$

$WF=1-CW*\cos(2*\pi*T/TI)$

"TIME WINDOW

$TM=\text{MOD}(T, 3*TP)$

$TW=0.75*(\text{IF } TM<TP \text{ OR } TM>2*TP \text{ THEN } 1 \text{ ELSE } 2)$

$YP1=\text{IF } YP>0 \text{ THEN } TW \text{ ELSE } 1$

"TREND ELIMINATION

DYNAMICS

$DYS=\text{IF } T<TI \text{ THEN } Y*S*WF*YP1 \text{ ELSE } 0$

"SINE CHANNEL

$DYC=\text{IF } T<TI \text{ THEN } Y*C*WF \text{ ELSE } 0$

"COSINE CHANNEL

A:1

"SIGNAL AMPLITUDE

W:1

"FREQUENCY [RAD/S]

NP:20

"NUMBER OF PERIODS

CW:0

"PUT CW:1 IF WINDOW DESIRED

YP:-1

"PUT YP>0 FOR TREND ELIMINATION

$\pi:3.1415926$

END

To study the frequency analyser it is necessary to simulate the system representing the process dynamics. The simple first order system with the transfer function $G(s) = 1/(1+s)$ is used in many of the examples. A program PROC to simulate this system is listed below. The interconnection between the process and the analyser is given by the system LINK1. This program also admits the possibility to simulate a disturbance in the process output of the form

$$n(t) = a + bt + c \sin(\omega t + \phi)$$

The program listings for PROC and LINK1 are given below.

CONTINUOUS SYSTEM PROC "PROCESS DYNAMICS

INPUT U
OUTPUT Y
STATE X
DER DX

OUTPUT
Y=X

DYNAMICS
DX=U-X

END

CONNECTING SYSTEM LINK1

TIME T

YSR=T/4
YCR=-T/4
ABSGR=1/SQRT(2)
ARGGR=-PI/4

Y[FREQA]=Y[PROC]+A+B*T+C*SIN(W*T+FI)
U[PROC]=U[FREQA]

A:0
B:0
C:0
W:0
FI:0
PI:3.1415926
PD:-1

END

The programs FREQA PROC and LINK1 can be used to get an insight into the properties of the frequency analyser. Some examples are given below.

Generation of Fig. 3.4 and solution of Exercise 3.7.

To generate Fig. 3.4 the following dialogue is carried out using SIMNON.

```
>SYST FREQA PROC LINK1  "GENERATE SYSTEMS TO BE SIMULATED
>PAR NP:2                "SET INTEGRATION TIME TO 2 PERIODS
>INIT X[PROC]:-0.5       "SET INITIAL STATE OF PROCESS
>AXES H 0 15 V -4 3      "SET SCALES FOR GRAPH
>PLOT Y[FREQA] U[FREQA]  "CHOOSE VARIABLES TO BE PLOTTED
>SIMU 0 13               "SIMULATE
>PLOT YS YC YSR YCR      "CHOOSE VARIABLES TO BE PLOTTED
>AXES
>SIMU
>PLOT ABSG ARGG ABSGR ARGGR
>AXES V -2 2
>SIMU
>
```

The programs FREQA PROC and LINK1 are conveniently used in order to find the effect of disturbances of the form (A1) on the results. For example, to find the effect of a sinusoidal perturbation, the following dialogue is carried out.

```
>SYST FREQA PROC LINK1  "ACTIVATE SYSTEMS TO BE SIMULATED
>PAR NP:10              "SET INTEGRATION TIME TO 10 PERIODS
>PAR C:1                "INTRODUCE SINUSOIDAL DISTURBANCE
>PAR W[LINK1]:1.1        "FREQUENCY OF DISTURBANCE 1.1 RAD/S
>AXES H 0 100 V -20 15
>PLOT YS YC YSR YCR
>SIMU 0 70
>PAR W[LINK1]-\:1.15
>SIMU
>PAR FI:0.7              "CHANGE PHASE OF DISTURBANCE
>SIMU
>PAR W[LINK1]:1.2
>PLOT YS YC
>SIMU -MARK
>
```

A3. Effects of Random Disturbances.

Random disturbances are conveniently generated using SIMNON because the language contains a white noise generator NOISE. A disturbance with an arbitrary spectral density can then be generated by filtering the white noise. This is accomplished by the system FILT. The necessary connections are given in the system LINK2. The programs FILT and LINK2 are listed below.

CONTINUOUS SYSTEM FILT

"NOISE FILTER

INPUT U
OUTPUT Y
STATE X
DER DX

OUTPUT
 $Y = KF * X$

DYNAMICS
 $DX = (U - X) / TF$

KF:0
TF:1

END

CONNECTING SYSTEM LINK2

TIME T

YSR=T/4
YCR=-T/4

U[FILT]=E1[NOISE]
U[PROC]=U[FREQA]
Y[FREQA]=Y[PROC]+Y[FILT]

END

Generation of Fig. 3.5B.

As an example of a simulation of the effect of random disturbances the dialogue used to generate Fig. 3.5B is given.

```

>SYST FREQA PROC FILT NOISE LINK2
>PAR DT:0.05           "SET SAMPLING INTERVAL FOR NOISE
>PAR R11:4             "SET NOISE COVARIANCE
>PAR KF:0.375          "SET FILTER GAIN
>PAR TF:0.1            "SET FILTER TIME CONSTANT
>AXES H 0 50 V -3 3
>PLOT Y(FREQA)
>SIMU 0 31.415926
>AXES V -7 7
>PLOT YS YC YSR YCR
>SIMU
>

```

A4. Trend Elimination.

The effect of trend disturbances in the process output can be eliminated using Persson's device as was described in Section 4. Mathematically the necessary operation is given by equation (4.4). The scheme can be implemented by multiplying the process output with the weights α_k which are constants for each half period. This facility is included in the frequency analyser FREQA. Trend elimination in the sine channel is activated by $YP > 0$.

To demonstrate trend elimination we give the following dialogue which was used to generate Fig. 4.1 and Fig. 4.2.

```
>SYST FREQA PROC LINK1
>PAR NP:12          "SET INTEGRATION TIME TO 12 PERIODS
>PAR B:0.1          "INTRODUCE TRED\ND ERROR IN PROCESS OUTPUT
>INIT X[PROC]:-0.5
>AXES H 0 100 V -40 30
>PLOT YS YC YSR YCR
>SIMU 0 80
>PAR YP:1           "INTRODUCE TREND ELIMINATION
>PLOT YS
>SIMU
>
```

